Earthquake source parameters from low-frequency normal mode data using the Neighbourhood Algorithm

K. Lentas[(1)], A. M. G. Ferreira[(1)], E. Clévédé[(2)]

[(1)]School of Environmental Sciences, University of East Anglia, Norwich, UK
[(2)]Institut du Globe de Physique, Paris, France

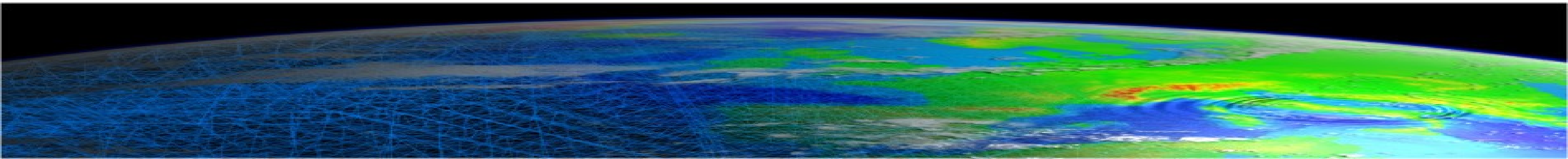

Goal and motivation

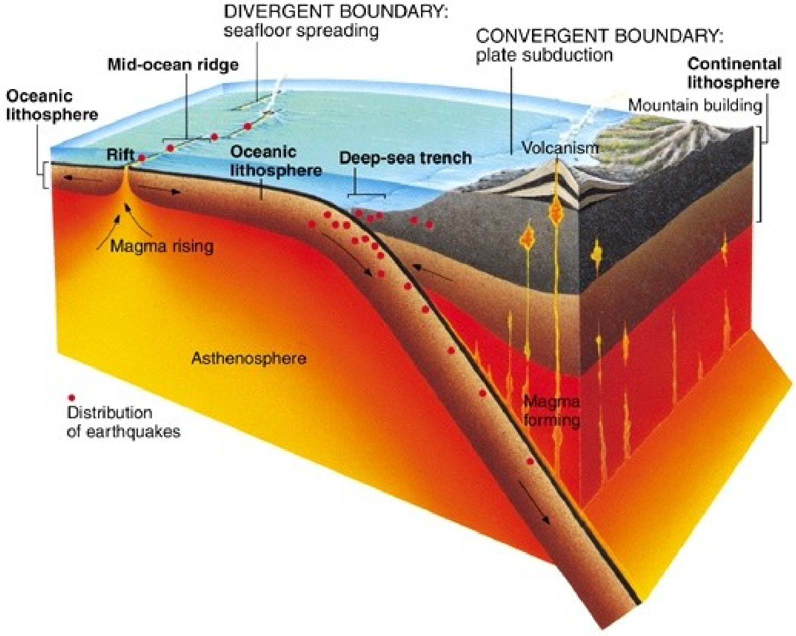

- Large magnitude – shallow earthquakes
- Tsunami excitation
- Finite character of the source
- Uncertainties in source parameters

Goal and motivation

Earth's free oscillations

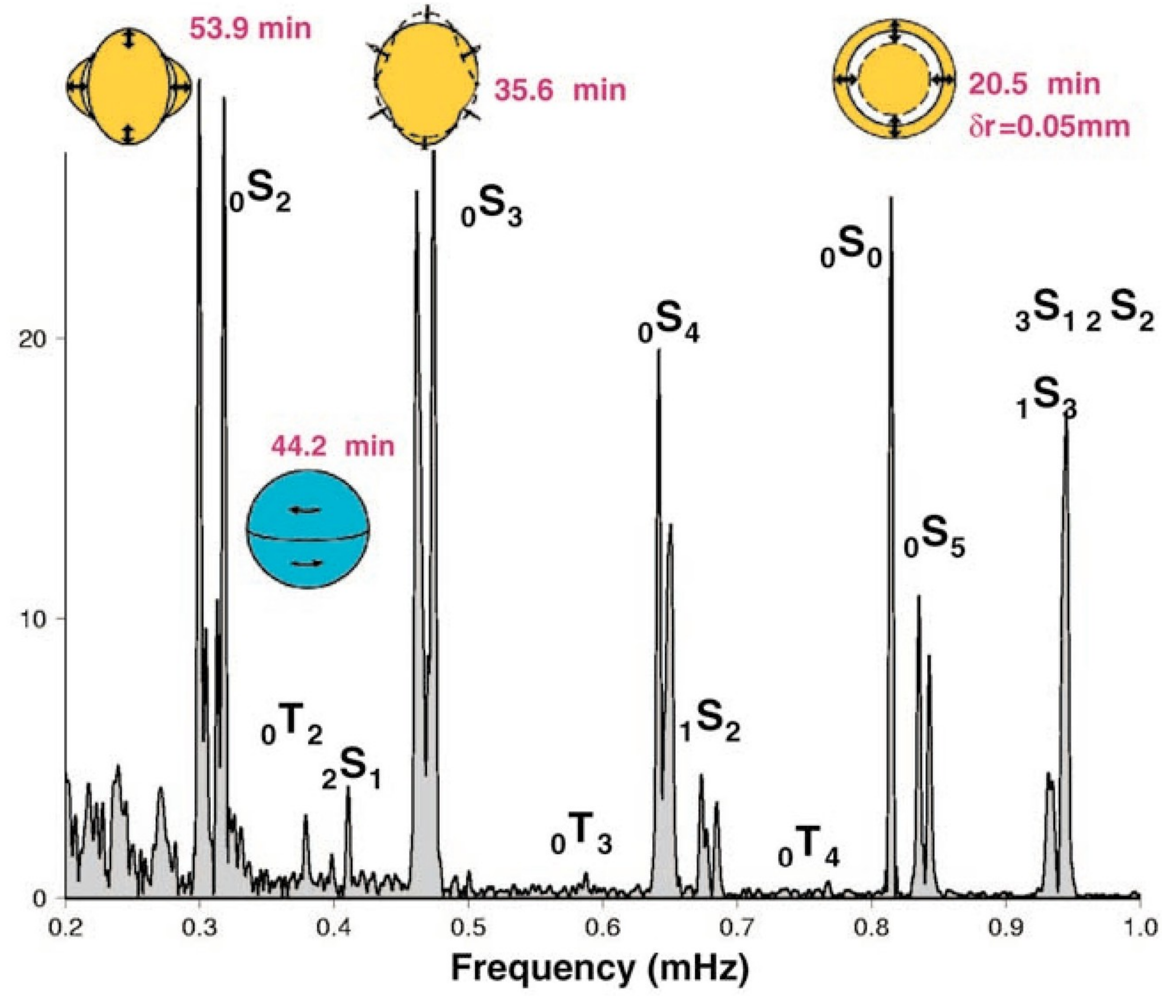

Park et al. (2005)

Earth's free oscillations

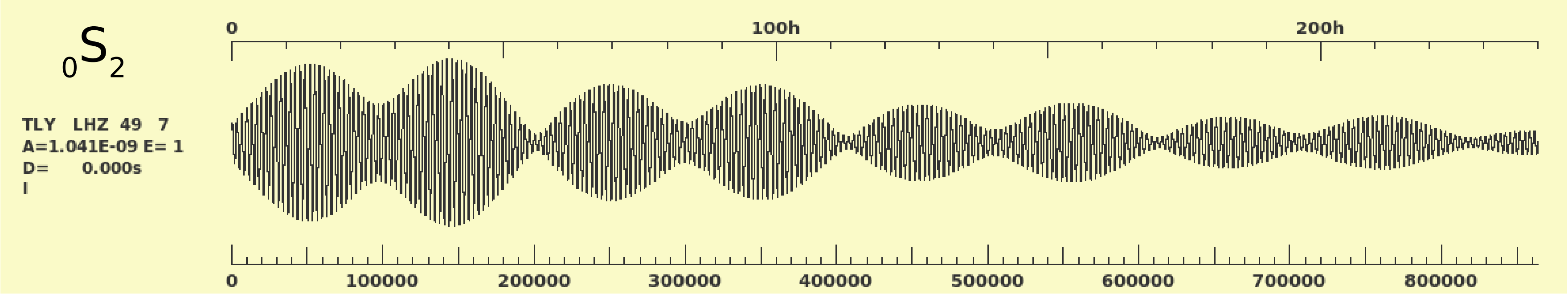

Earth's free oscillations

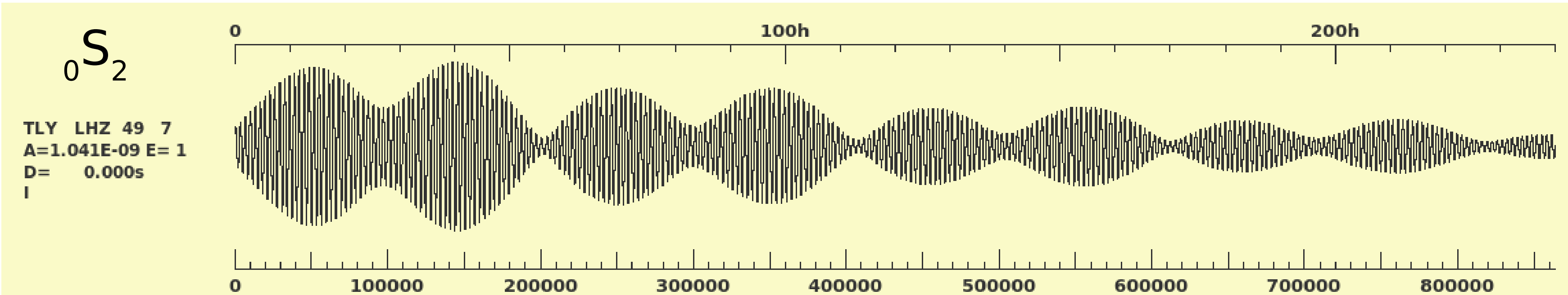

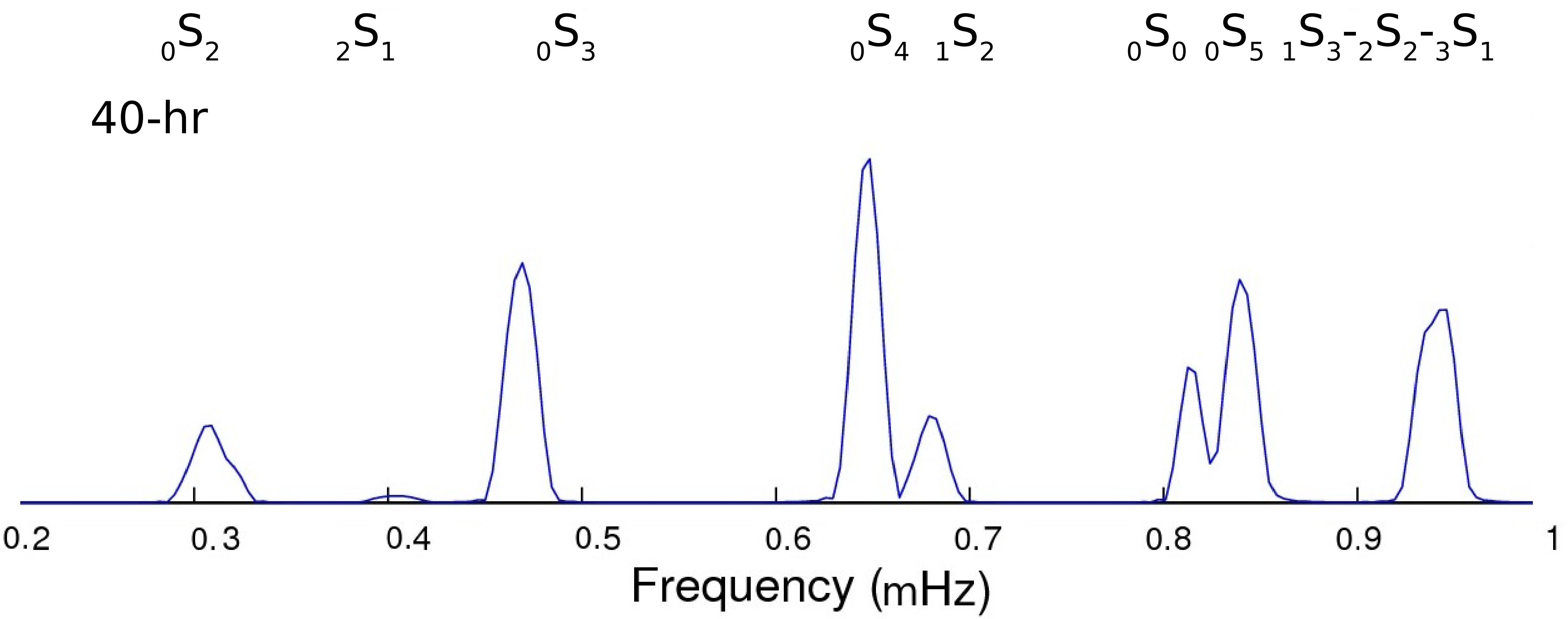

Earth's free oscillations

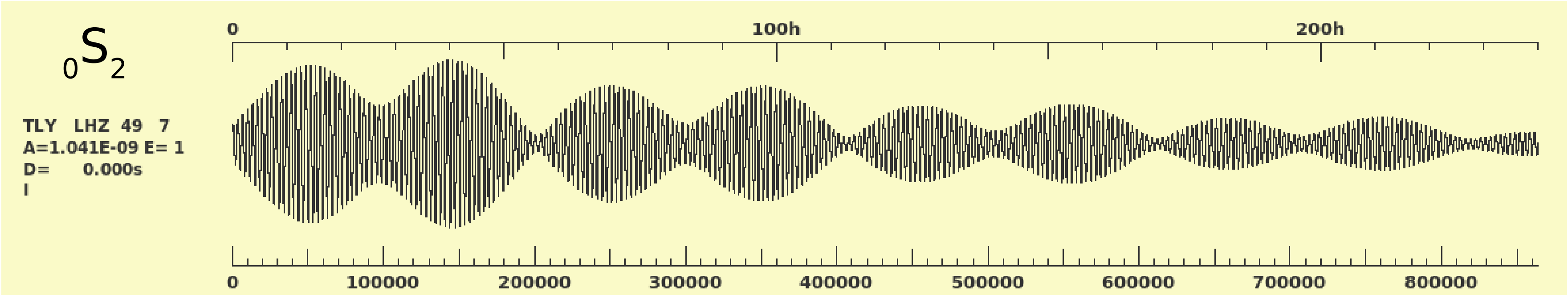

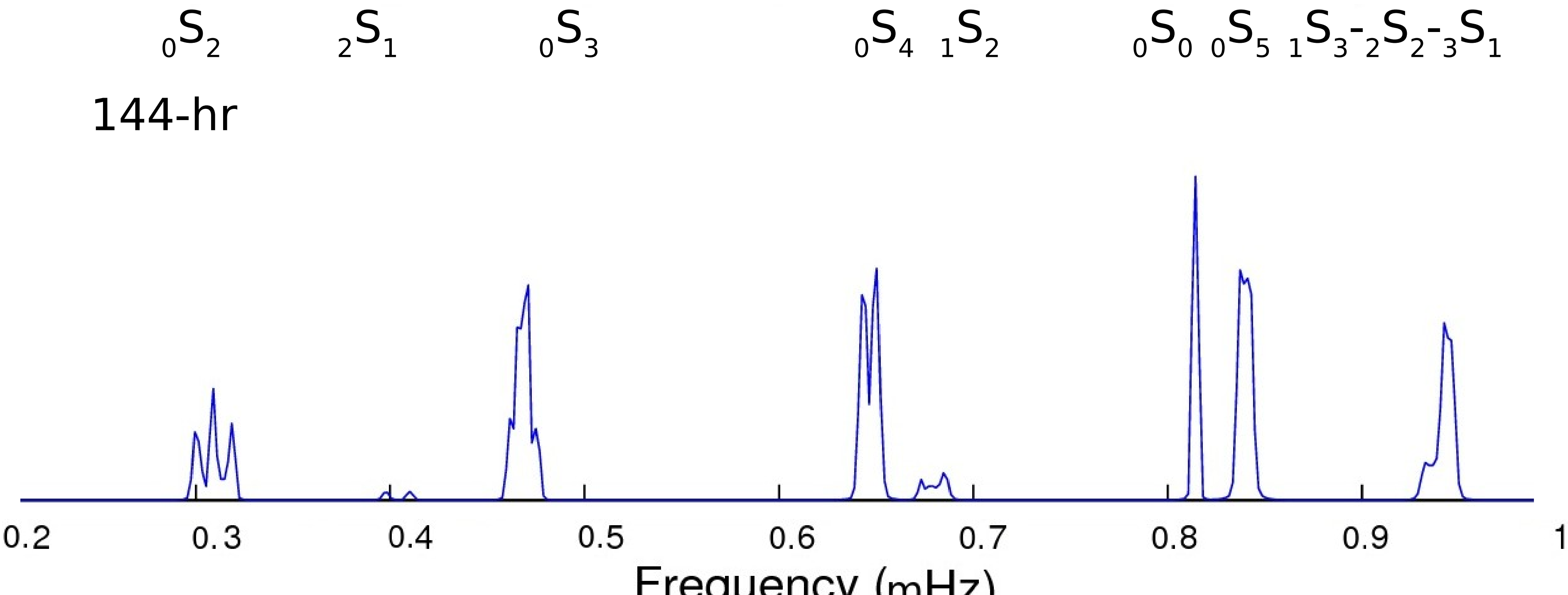

Earth's free oscillations

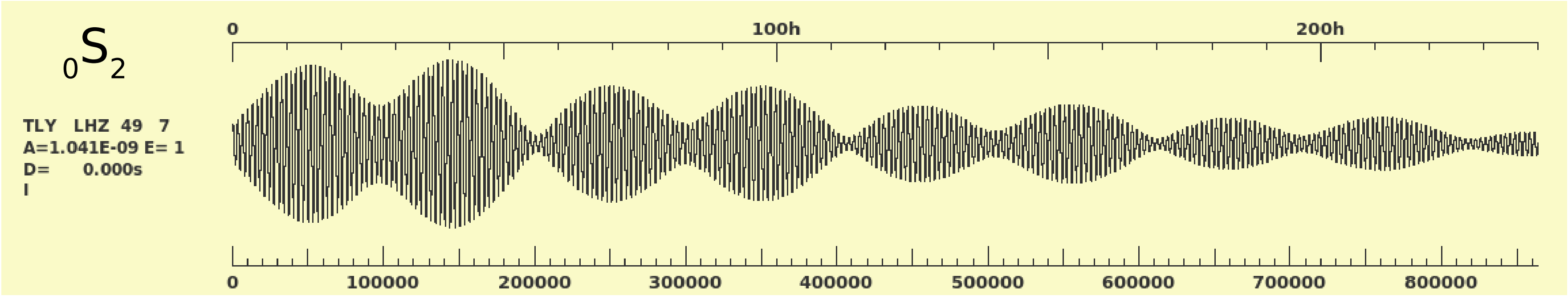

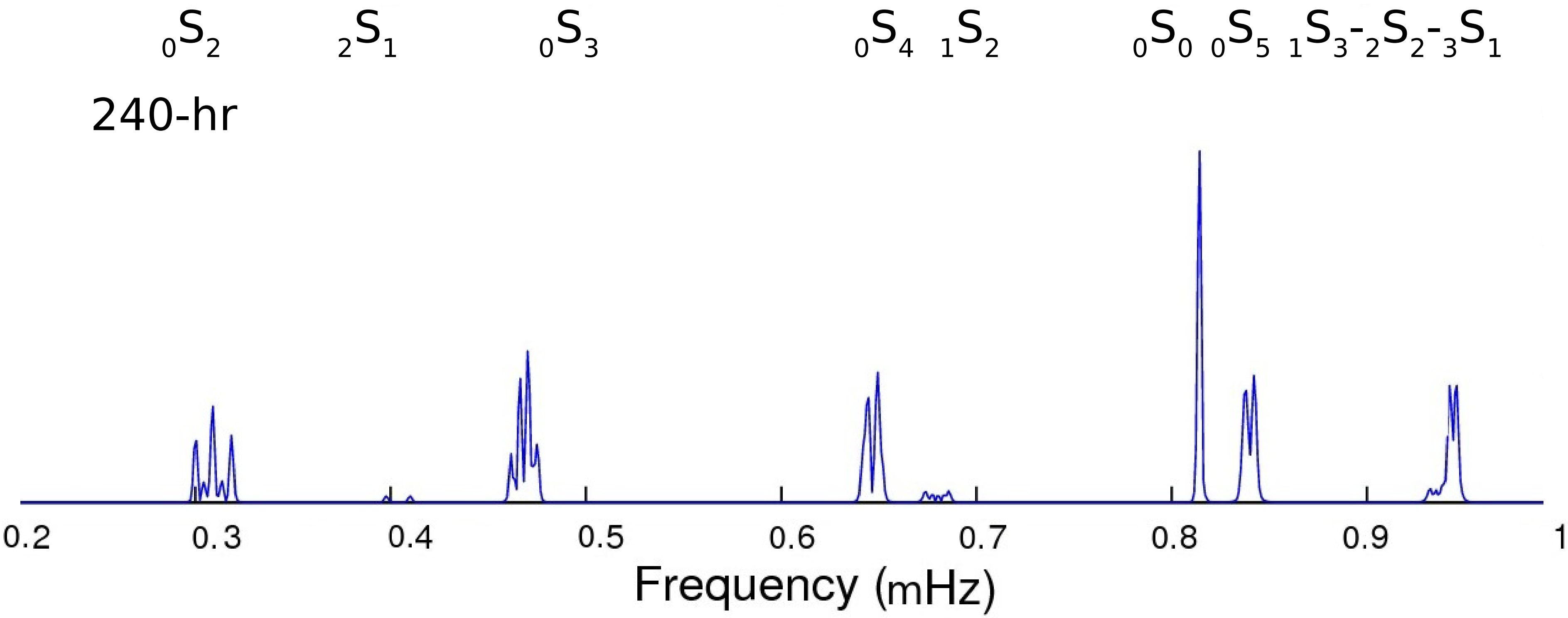

Finite source description

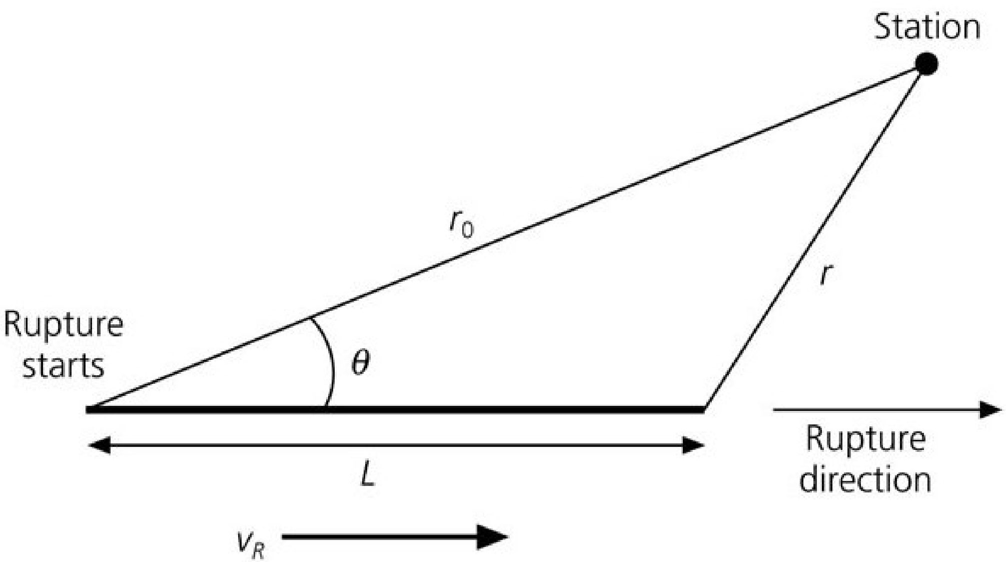

$$a^m_{fs}(x,\omega)=a^m_{ps}(x,\omega)\cdot F_m$$

Finite source description

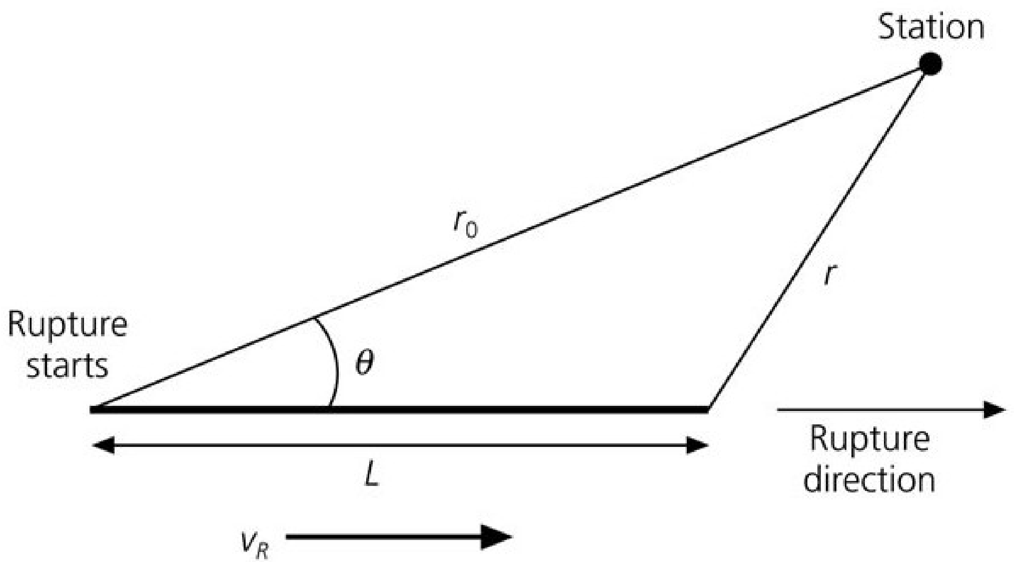

$$a_{fs}^{m}(x,\omega) = a_{ps}^{m}(x,\omega) \cdot F_m$$

$$a_{fs}^{m}(x,\omega) = \sum_{i=1}^{6} \left(\psi_i^m(x,\omega) \cdot M_i \right) \cdot F_m$$

Finite source description

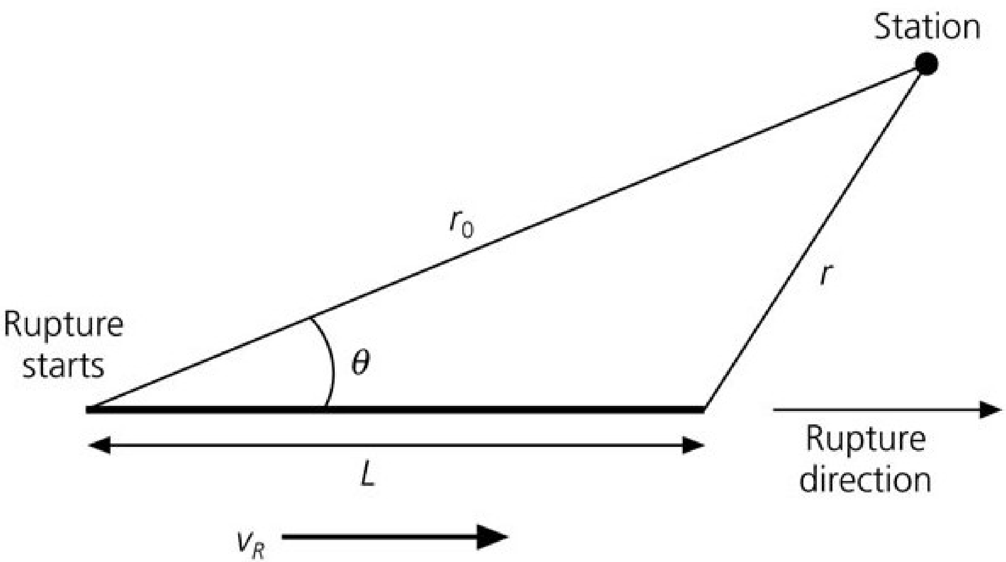

$$a^m_{fs}(x,\omega) = a^m_{ps}(x,\omega)\cdot F_m$$

$$a^m_{fs}(x,\omega) = \sum_{i=1}^{6} (\psi^m_i(x,\omega) \cdot M_i) \cdot F_m$$

$$F_m = \frac{sin(X_m)}{X_m} e^{-iX_m}$$

$$X_m = f(L, T_r)$$

Finite source description

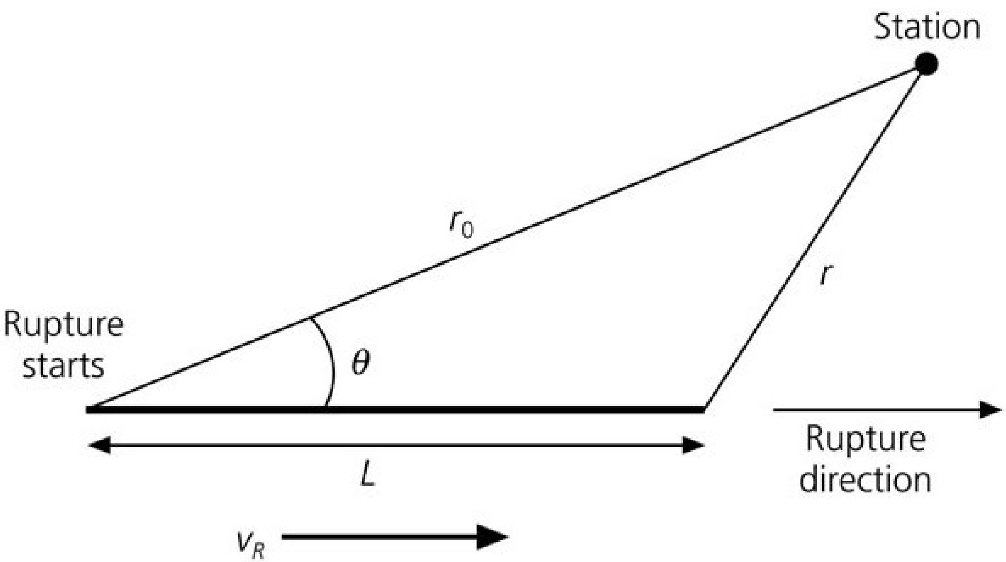

$$a^{m}_{fs}(x,\omega) = a^{m}_{ps}(x,\omega)\cdot F_{m}$$

$$a^{m}_{fs}(x,\omega) = \sum_{i=1}^{6}\left(\psi^{m}_{i}(x,\omega)\cdot M_i\right)\cdot F_m$$

$$F_m = \frac{sin(X_m)}{X_m}e^{-iX_m}$$

$$X_m = f(L, T_r)$$

Average
Rupture
Velocity

Probabilistic normal mode source inversion

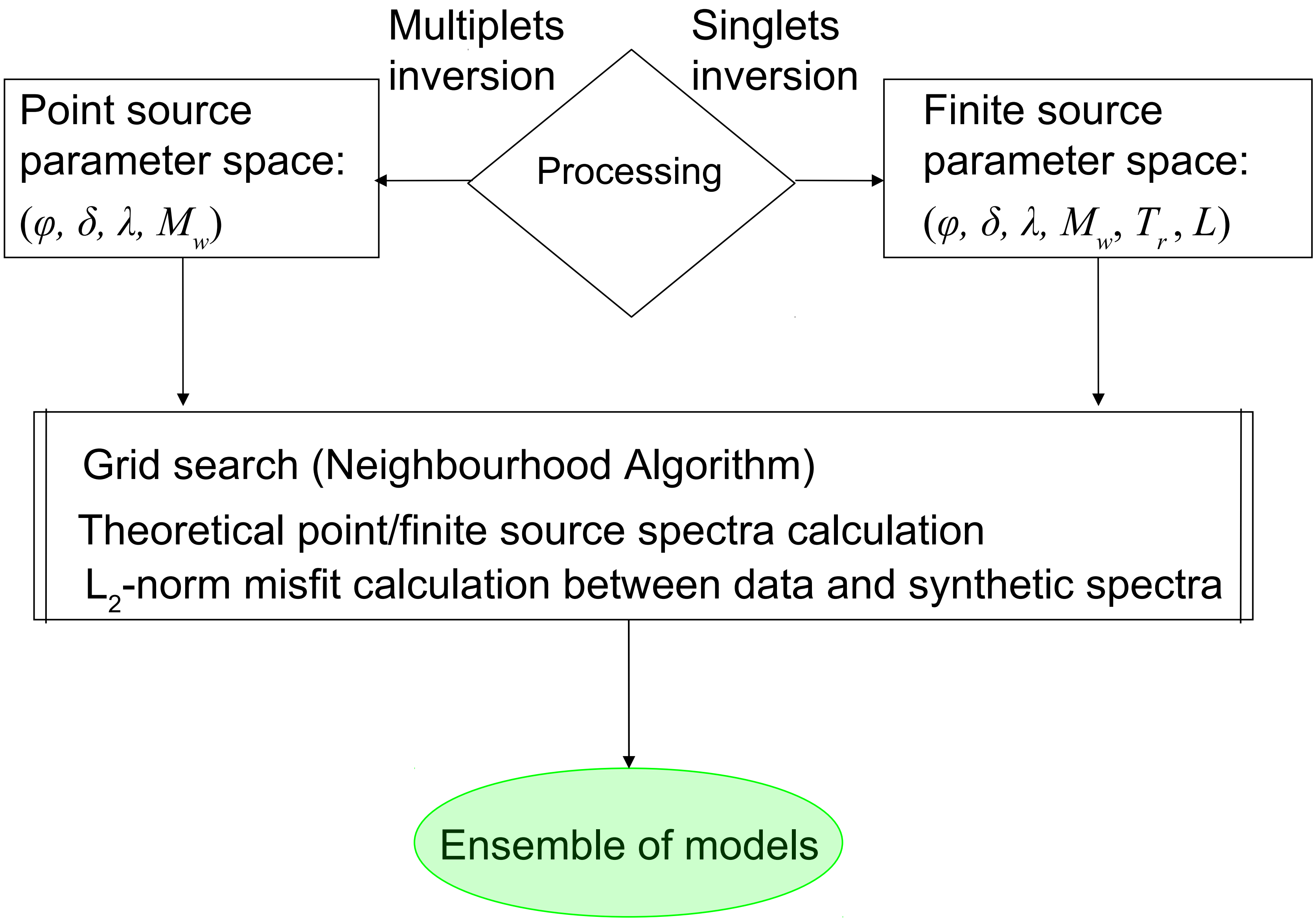

Synthetic tests

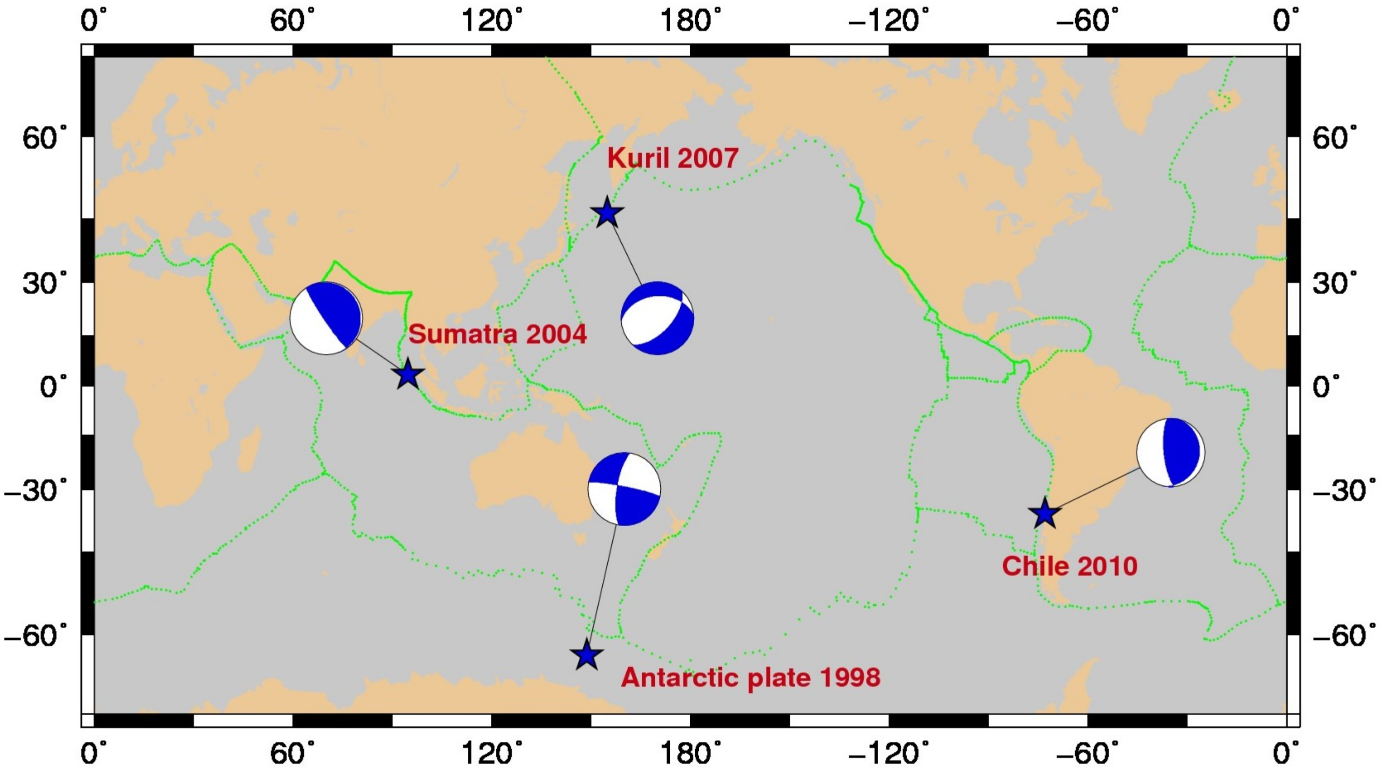

- Neglecting the finiteness of the source
- Noise in data
- Earth's structure
- Location and origin time errors

Synthetic tests

M_w=9.3
(T_r, L)=(545s,1140km)
Tsai et al. (2005)

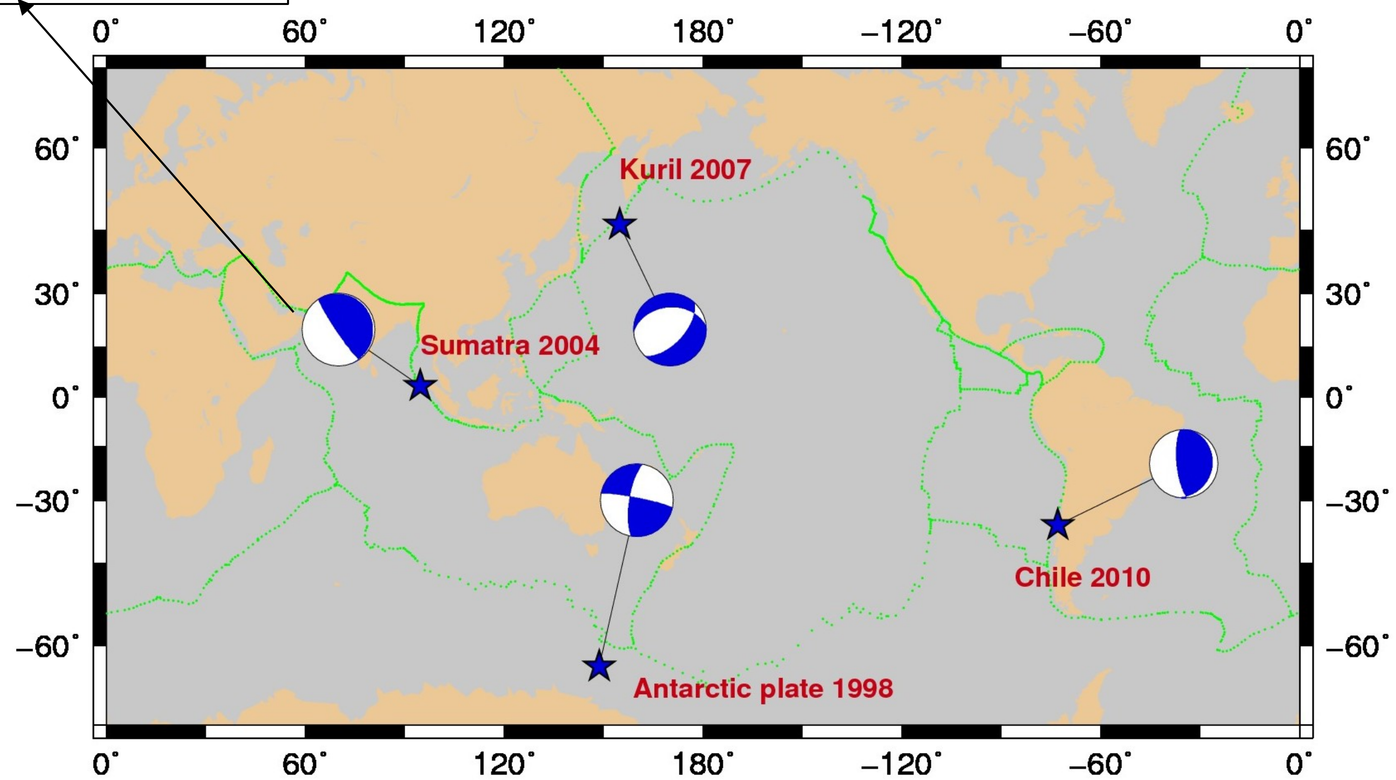

- Neglecting the finiteness of the source
- Noise in data
- Earth's structure
- Location and origin time errors

Synthetic tests

M_w=9.3
(T_r, L)=(545s,1140km)
Tsai et al. (2005)

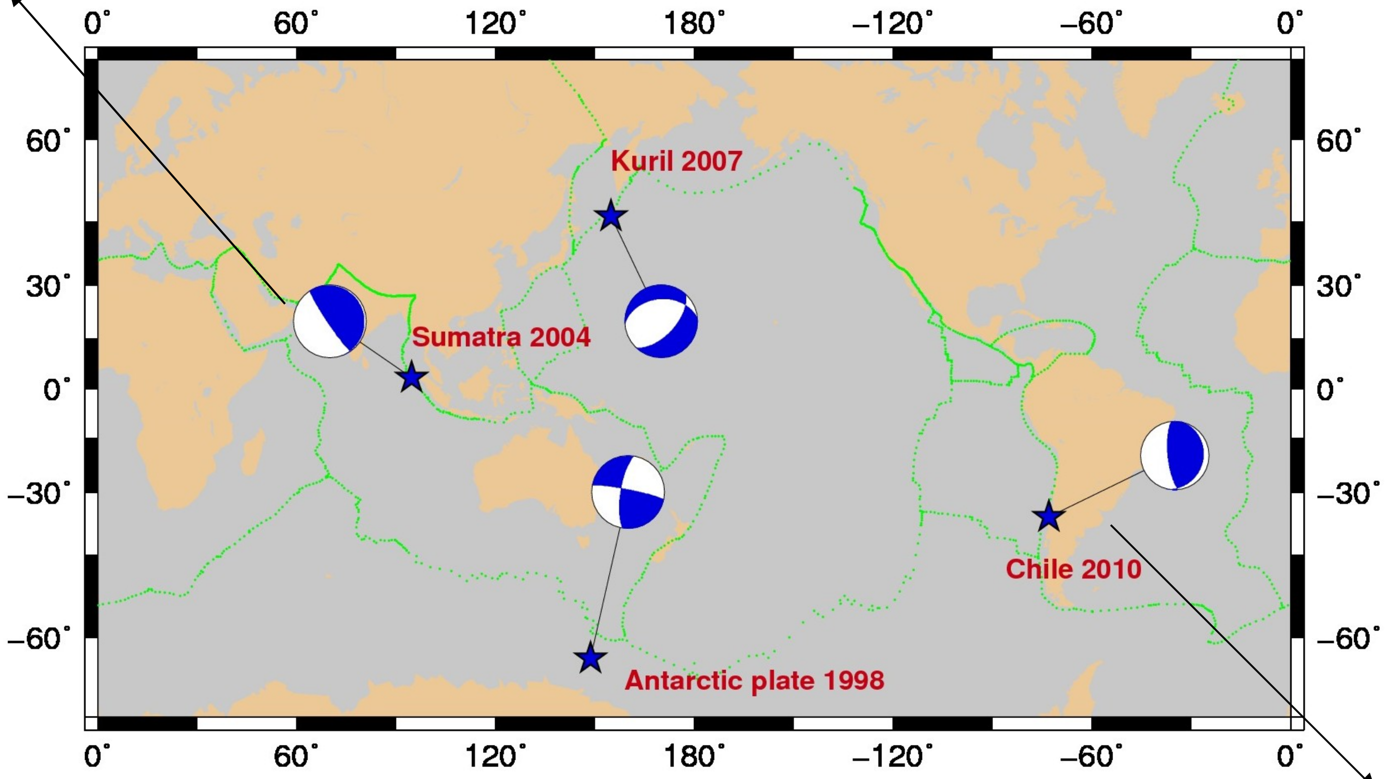

M_w=8.8
(T_r, L)=(230s,600km)
Delouis et al. (2011)

- Neglecting the finiteness of the source
- Noise in data
- Earth's structure
- Location and origin time errors

Synthetic tests

M_w=9.3
(T_r,L)=(545s,1140km)
Tsai et al. (2005)

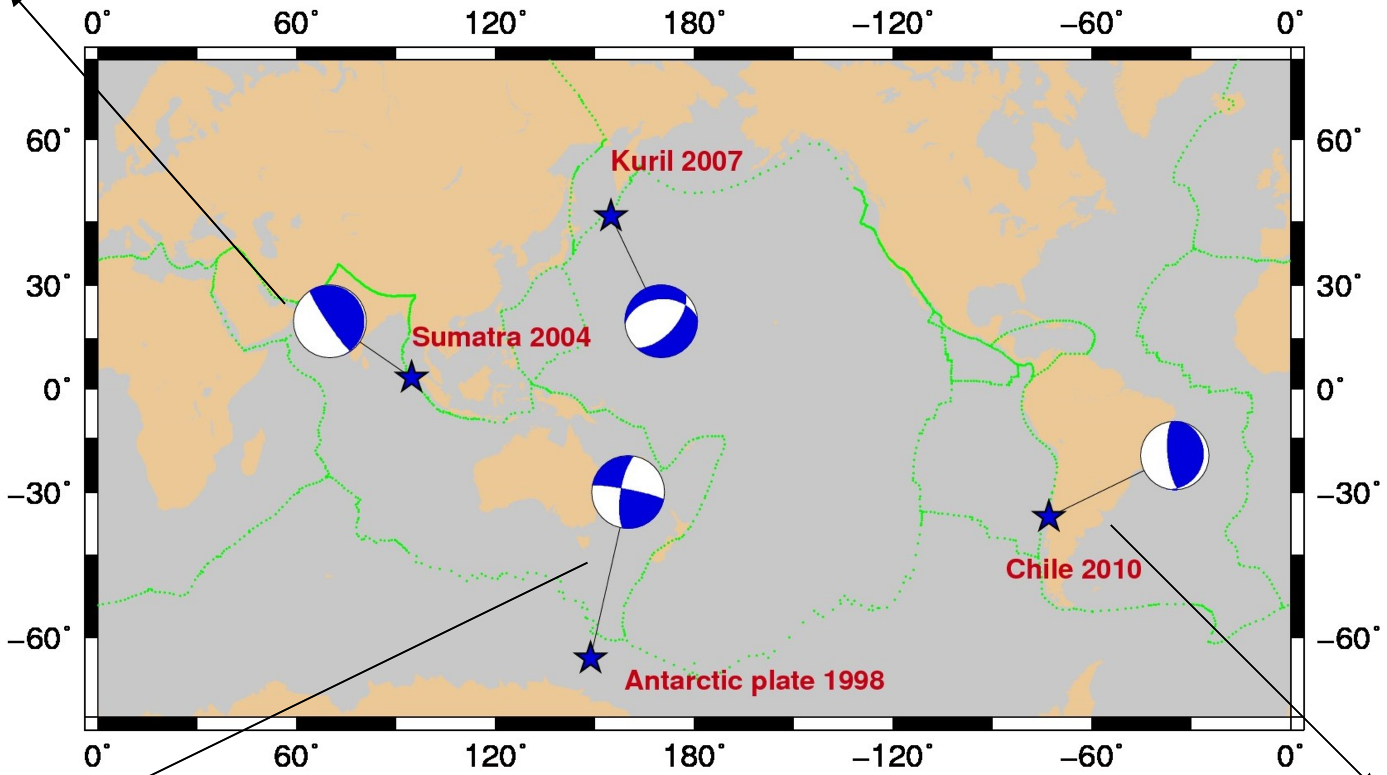

M_w=8.1
(T_r,L)=(90s,240km)
Nettles et al. (1999)

- Neglecting the finiteness of the source
- Noise in data
- Earth's structure
- Location and origin time errors

M_w=8.8
(T_r,L)=(230s,600km)
Delouis et al. (2011)

Synthetic tests

M_w=9.3
(T_r, L)=(545s,1140km)
Tsai et al. (2005)

M_w=8.1
(T_r, L)=(60s,220km)
Lay et al. (2009)

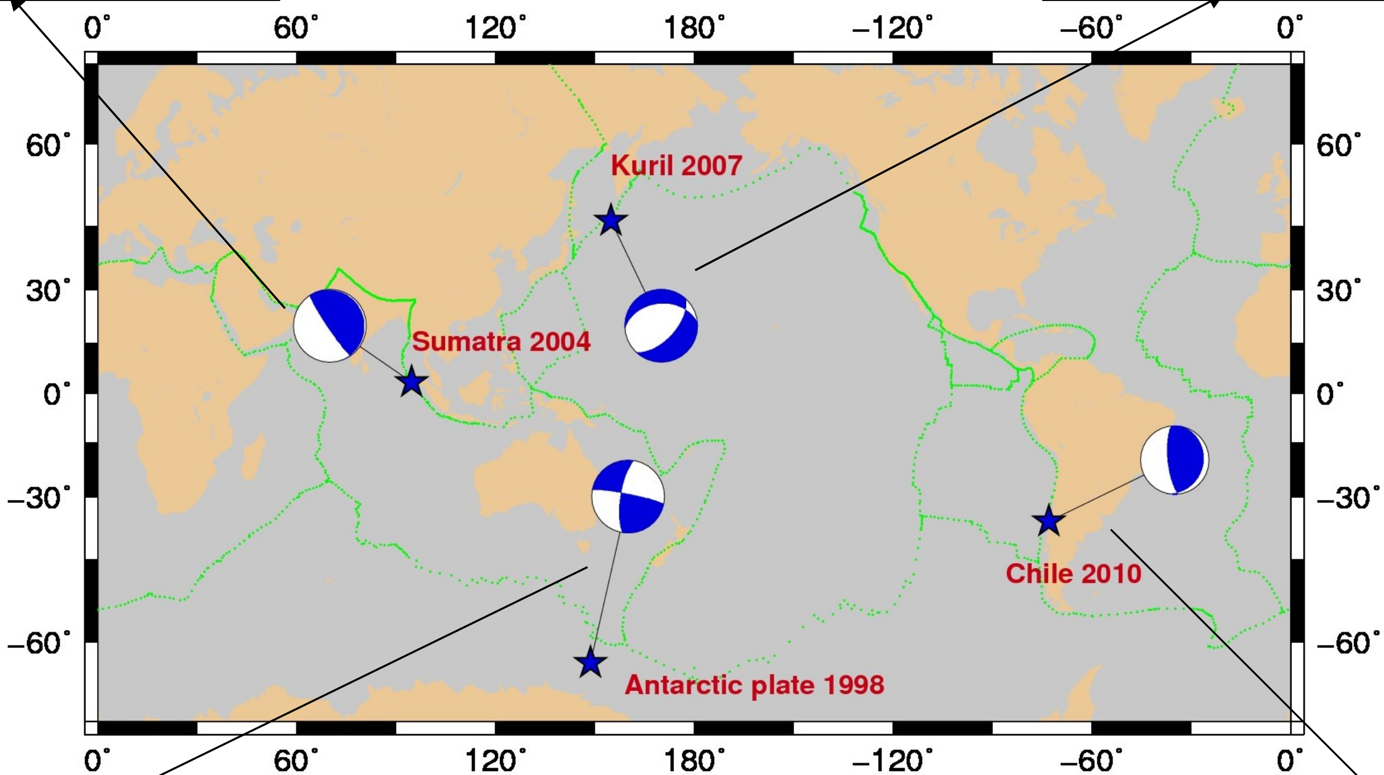

M_w=8.1
(T_r, L)=(90s,240km)
Nettles et al. (1999)

M_w=8.8
(T_r, L)=(230s,600km)
Delouis et al. (2011)

- Neglecting the finiteness of the source
- Noise in data
- Earth's structure
- Location and origin time errors

Synthetic tests (Sumatra 2004 M_w9.3 based on model of Tsai et al.(2005))

Combined effect of finiteness
and noise in synthetic data

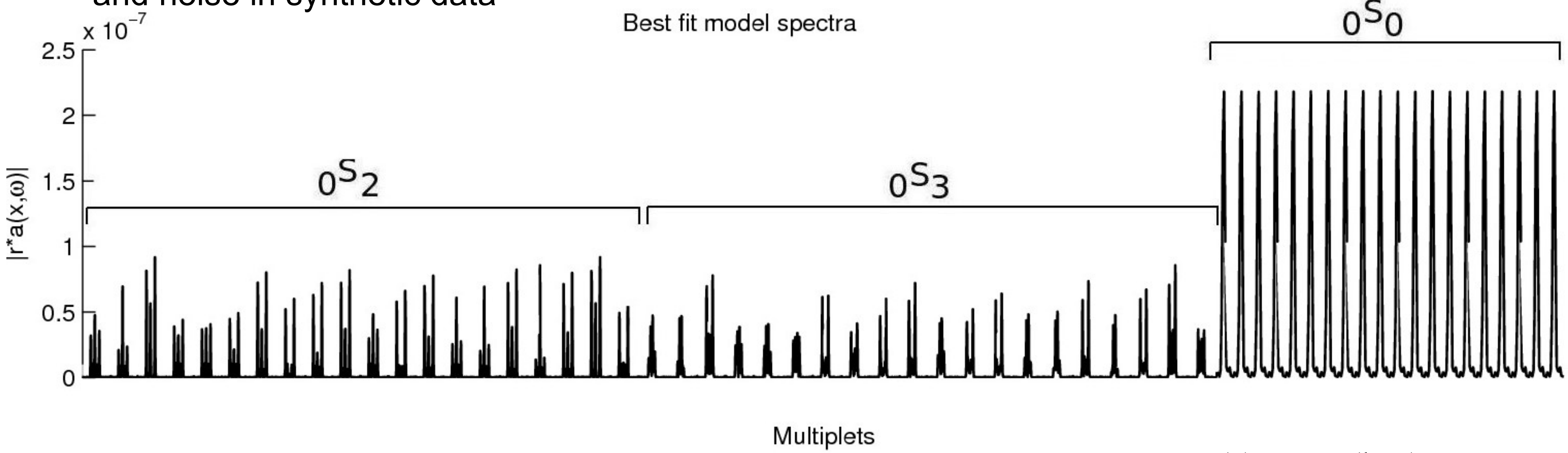

	$\varphi(^o)$	$\delta(^o)$	$\lambda(^o)$	M_w	T_r(s)	L (km)
Input model	343.00	6.10	107.00	9.31	545.00	1140.00

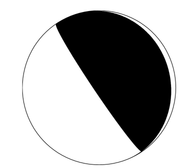

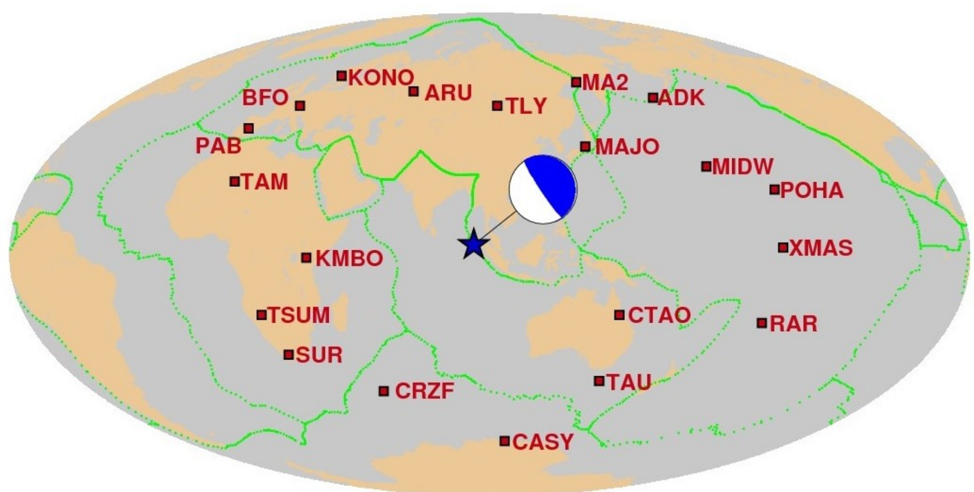

Synthetic tests (Sumatra 2004 M_w9.3 based on model of Tsai et al.(2005))

Combined effect of finiteness
and noise in synthetic data

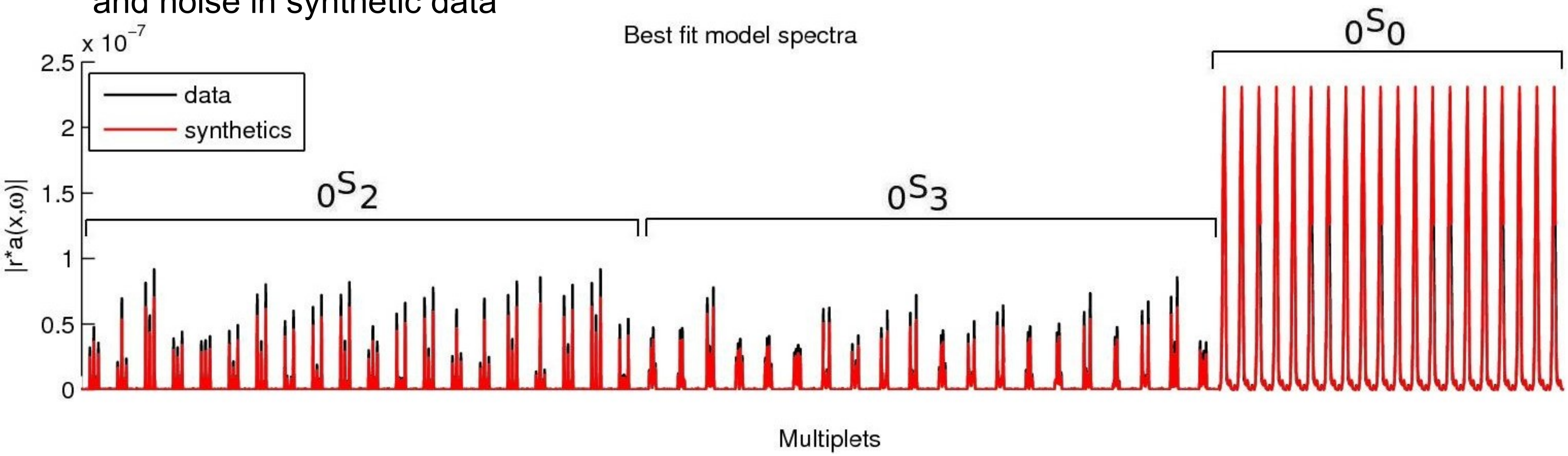

	$\varphi(^o)$	$\delta(^o)$	$\lambda(^o)$	M_w	T_r(s)	L (km)
Input model	343.00	6.10	107.00	9.31	545.00	1140.00
Optimal model	350.94	6.25	132.78	9.29		
Acceptable range	330.59-352.96	5.17-9.45	109.23-136.91	9.16-9.31		

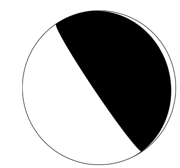

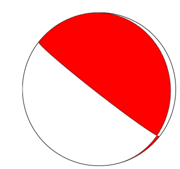

Min. misfit: 0.0561

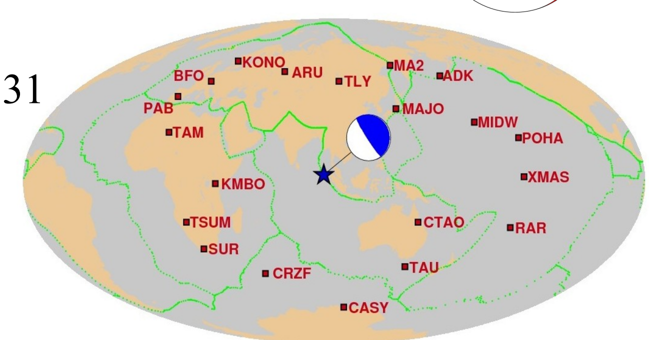

Synthetic tests (Sumatra 2004 M_w9.3 based on model of Tsai et al.(2005))

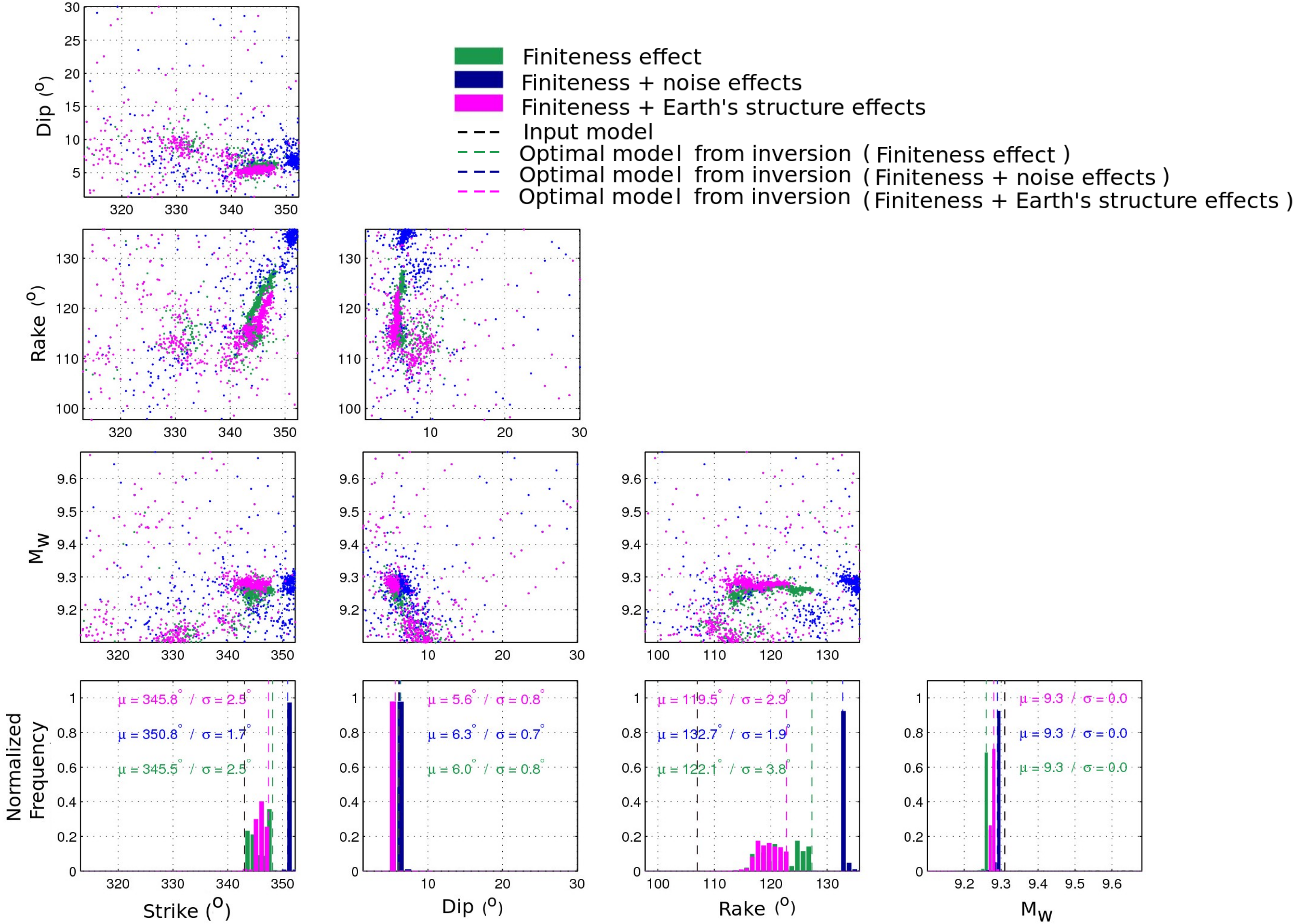

Synthetic tests (Sumatra 2004 M_w9.3 based on model of Tsai et al.(2005))

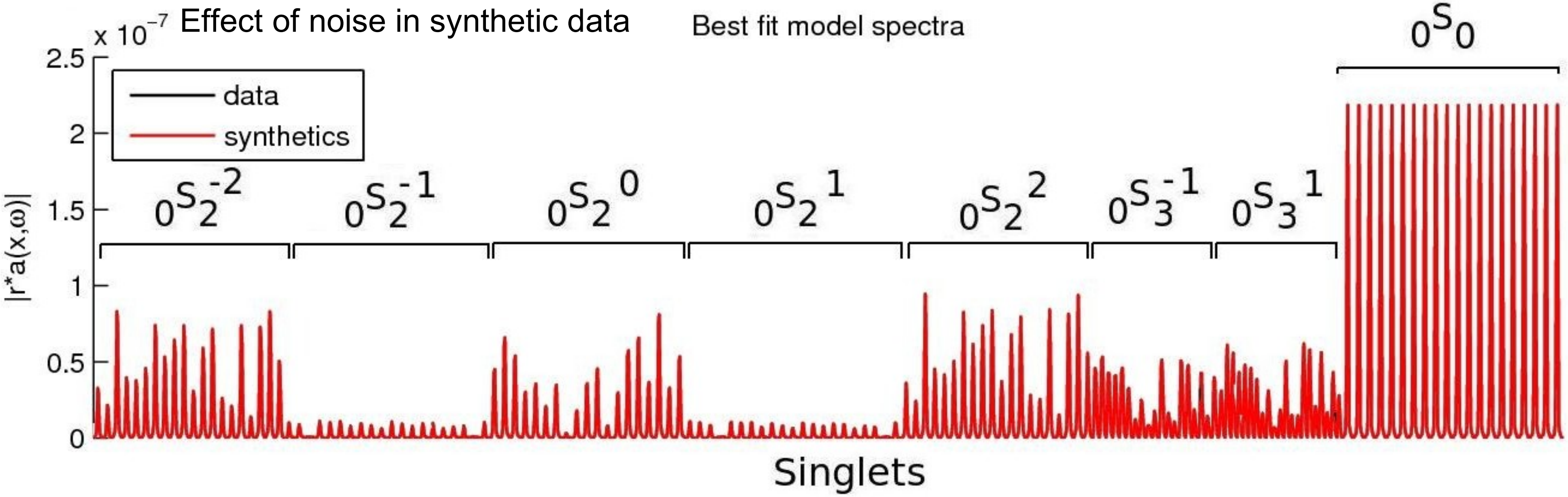

	φ(°)	δ(°)	λ(°)	M_w	T_r(s)	L (km)
Input model	343.00	6.10	107.00	9.31	545.00	1140.00
Optimal model	343.76	7.82	109.17	9.24	544.97	1119.68
Acceptable range	343.73-344.18	7.82-9.81	109.15-110.17	9.18-9.24	544.79-545.28	1116.28-1120.20

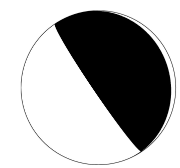

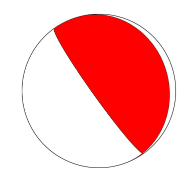

Min. misfit: 0.0000145

Synthetic tests (Sumatra 2004 M_w9.3 based on model of Tsai et al.(2005))

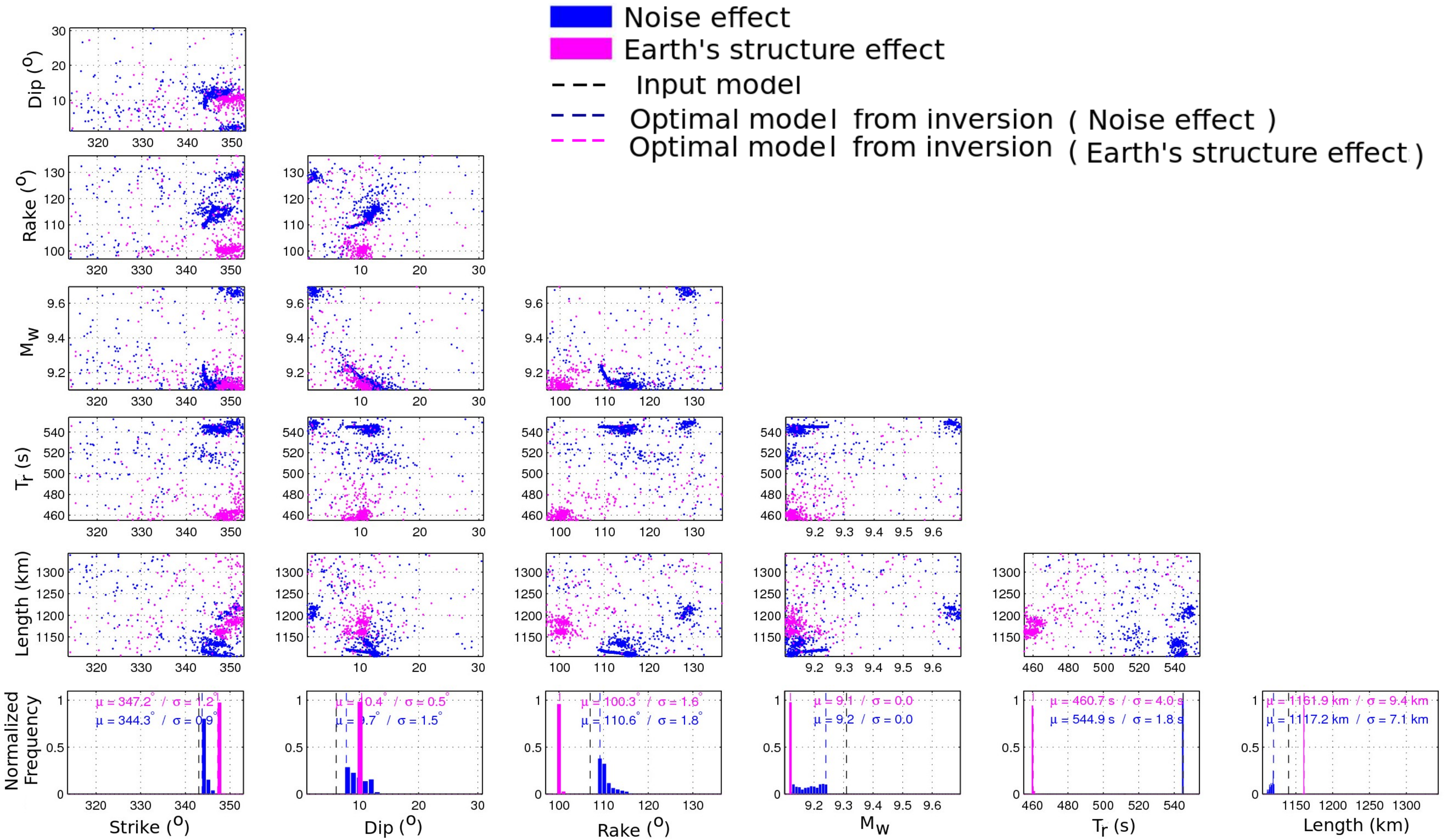

Synthetic tests

- Errors due to the neglecting of the finiteness of the source affect gradually the rake angle (up to 20^o) with respect to rupture dimensions.
- Up to 8^o error in fault geometry because of noise in data.
- Up to 150s error in rupture time because of Earth structure effect.
- Large location errors (1^o) can yield large errors in rake angle (up to 14^o).
- The rake angle is difficult to be constrained.
- Surprisingly the M_o-δ trade-off is relatively well resolved.

Application to real earthquakes

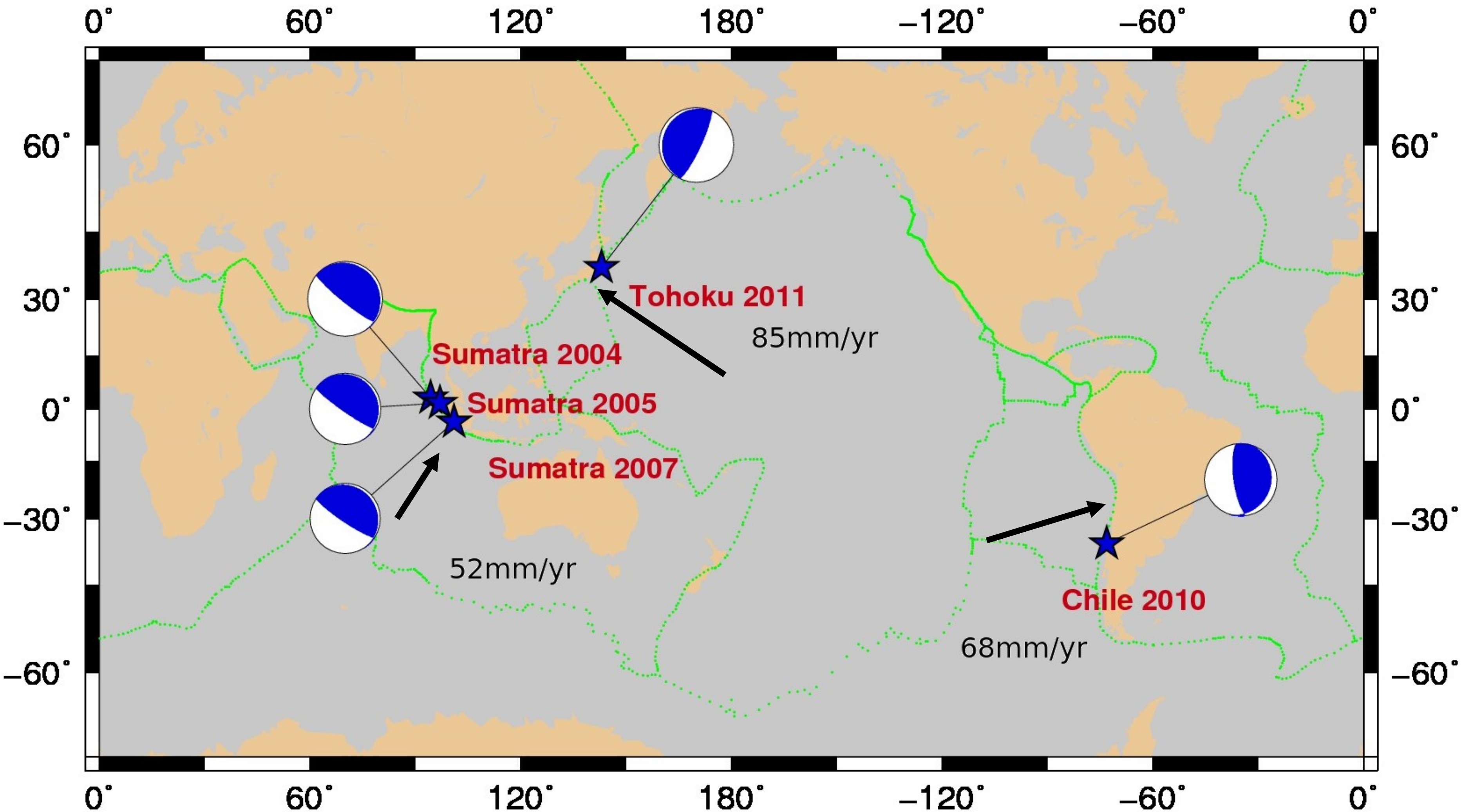

Application to real earthquakes (Sumatra 2004)

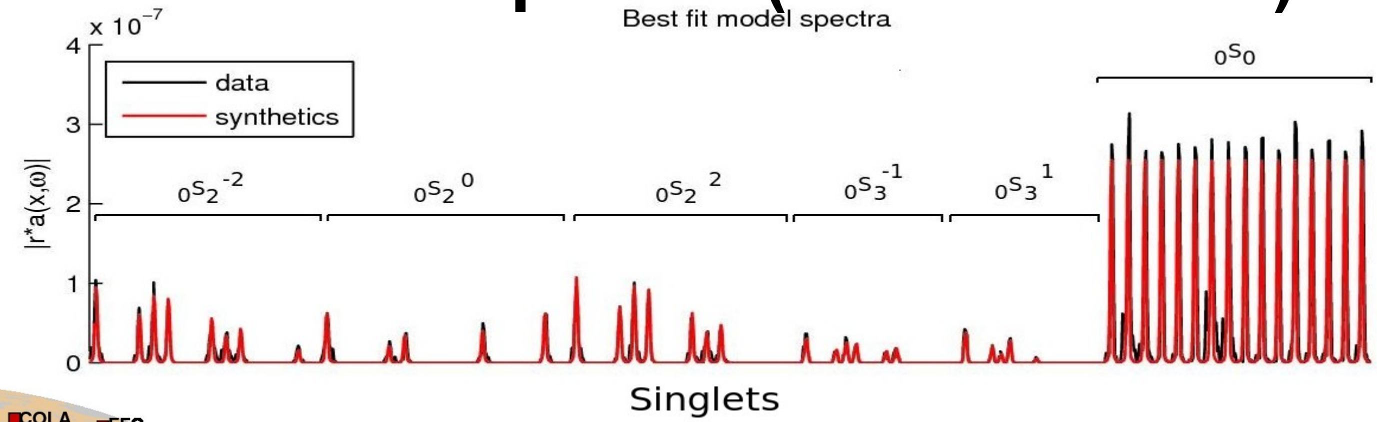

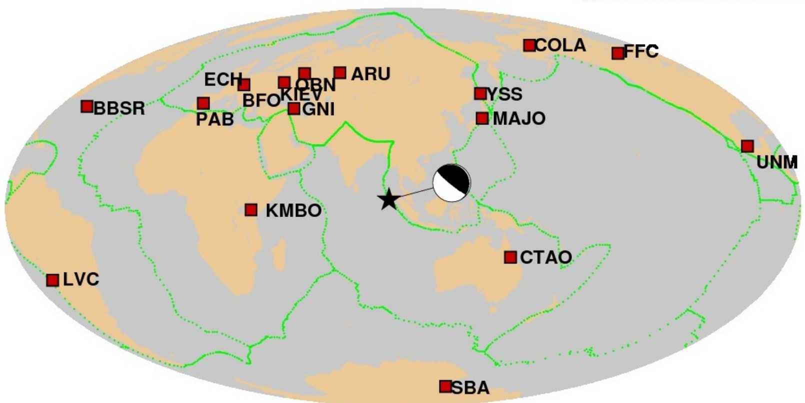

Min. misfit: 0.2463

	$\varphi(^o)$	$\delta(^o)$	$\lambda(^o)$	M_w	T_r (s)	L (km)	
Tsai et al. (2005)	343.00	6.10	107.00	9.31	545.00	1140.00	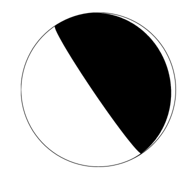
Optimal model	340.91	8.15	102.77	9.26	521.01	1276.77	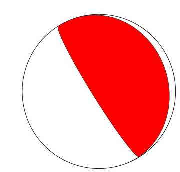
Acceptable range	309.02-346.77	6.92-30.35	90.50-115.70	8.92-9.30	480.08-544.33	1122.63-1322.51	

Application to real earthquakes (Sumatra 2004)

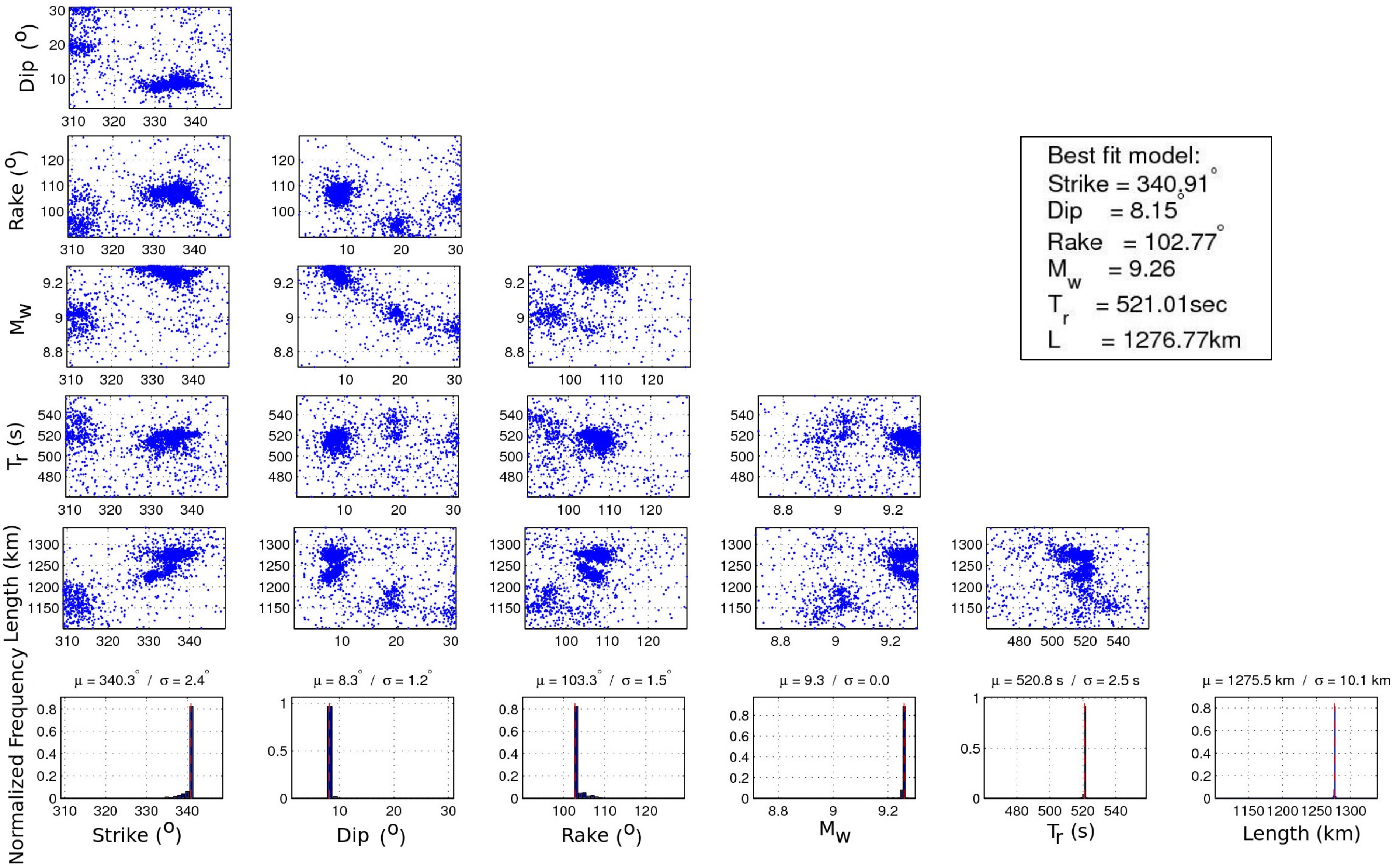

Best fit model:
Strike = 340.91°
Dip = 8.15°
Rake = 102.77°
M_w = 9.26
T_r = 521.01sec
L = 1276.77km

Application to real earthquakes (Tohoku 2011)

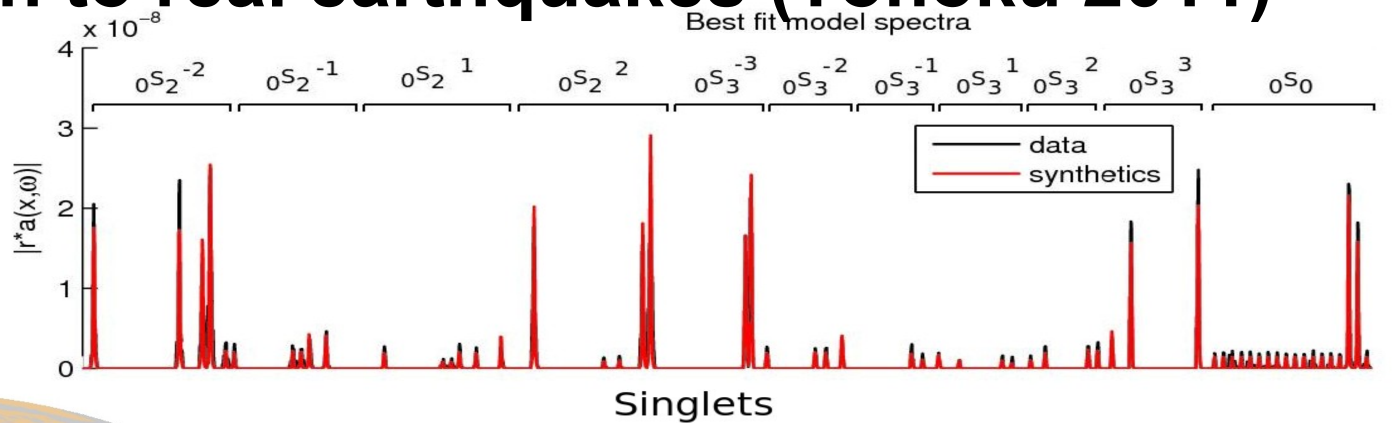

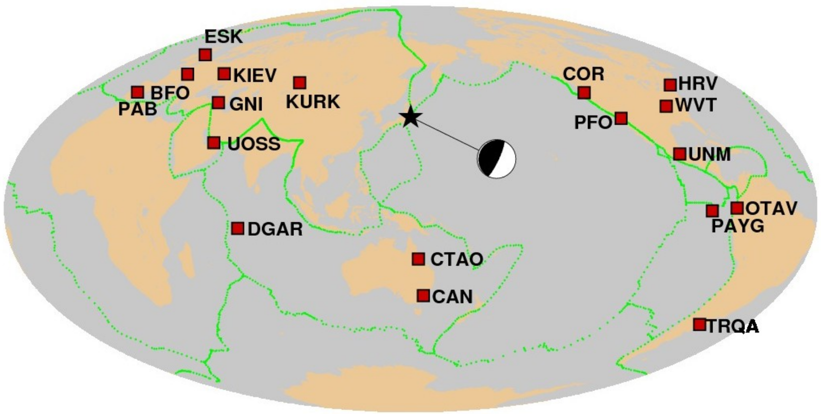

Min. misfit: 0.18028

	$\varphi(^{o})$	$\delta(^{o})$	$\lambda(^{o})$	M_w	T_r(s)	L (km)	
GCMT	203.00	10.00	88.00	9.10			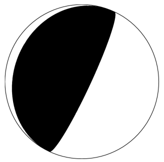
Optimal model	197.32	9.11	79.33	9.00	150.95	461.01	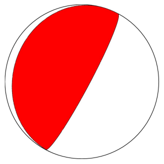
Acceptable range	189.06-209.14	8.96-19.78	68.17-102.18	8.80-9.00	133.47-197.22	448.49-559.03	

Application to real earthquakes (Chile 2010)

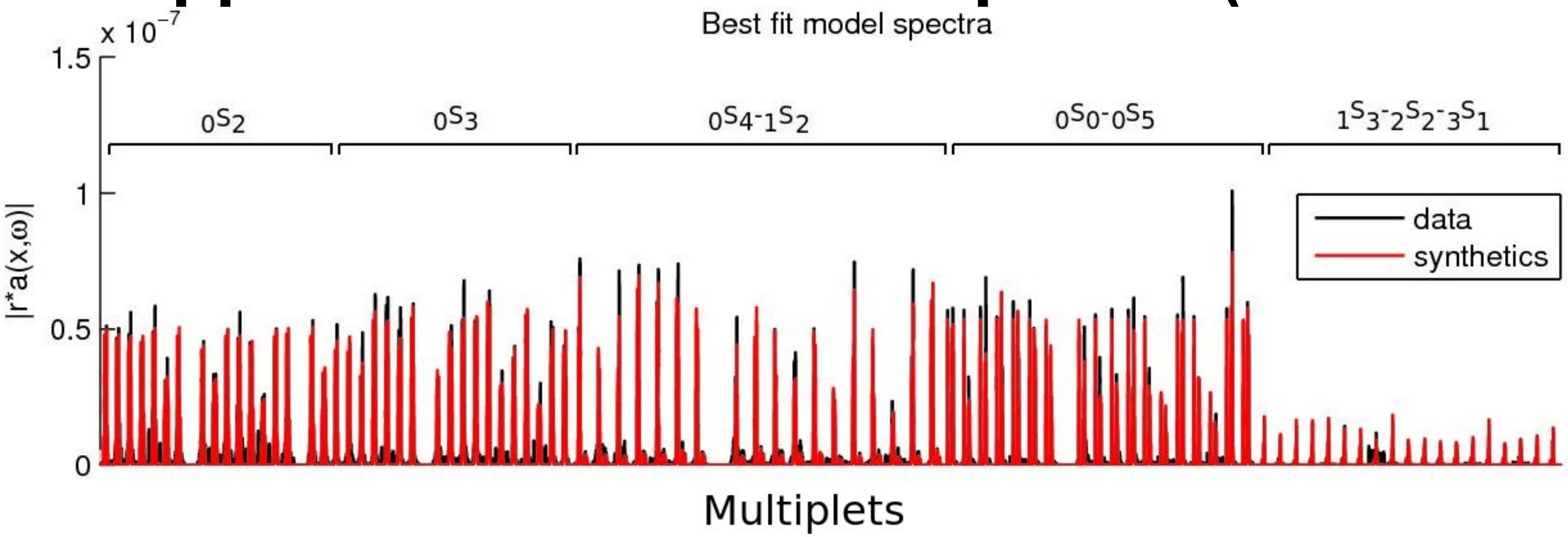

	$\varphi(^o)$	$\delta(^o)$	$\lambda(^o)$	M_w
GCMT	19.00	18.00	116.00	8.80
Optimal model	13.59	14.83	110.45	8.83
Acceptable range	8.55-20.40	11.99-21.92	109.02-119.44	8.74-8.89

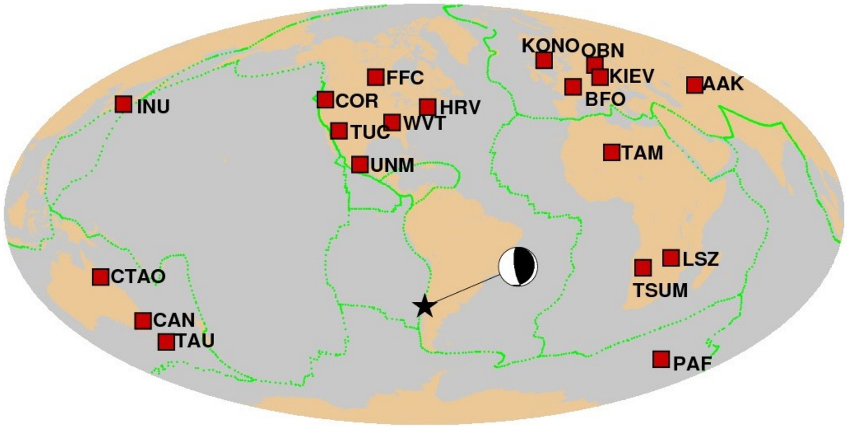

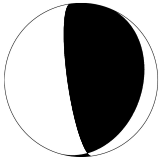

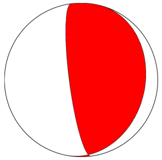

Min. misfit: 0.10344

Application to real earthquakes

$(\varphi,\delta,\lambda)=(341^o,8^o,103^o)$
$(M_w,T_r,L)=(9.3,521s,1277km)$

$(\varphi,\delta,\lambda)=(197^o,9^o,79^o)$
$(M_w,T_r,L)=(9.0,151s,461km)$

$(\varphi,\delta,\lambda)=(341^o,9^o,133^o)$
$(M_w,T_r,L)=(8.7, -, -)$

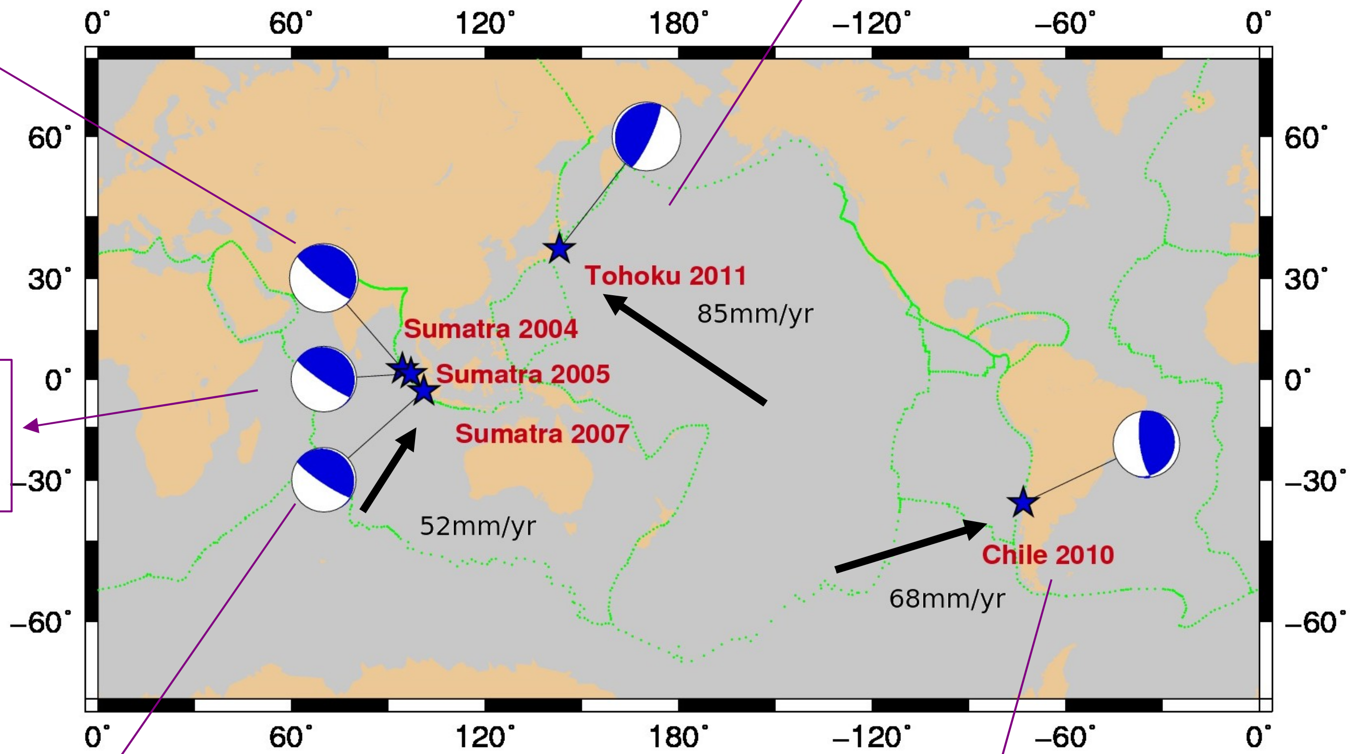

$(\varphi,\delta,\lambda)=(330^o,8^o,112^o)$
$(M_w,T_r,L)=(8.6, - , -)$

$(\varphi,\delta,\lambda)=(14^o,15^o,111^o)$
$(M_w,T_r,L)=(8.8, -, -)$

Conclusions

- The neglect of finite rupture effects yields errors in rake gradually as the rupture dimensions (T_r, L) increase.
- Noise is not a significant source of errors in source parameters.
- The use of simplified 1D Earth model can lead to considerable errors in fault geometry (up to 8^o) and large errors in rupture time (up to 150s) and length (up to 140km).
- Spatio-temporal location uncertainties yield considerable errors in rake angle (up to 14^o) and rupture length (~190km).
- We successfully determined simultaneously the fault geometry, moment magnitude and rupture characteristics of the giant 2004 Sumatra and 2011 Tohoku earthquakes.
- Normal mode data can offer an independent way to study large seismic sources and highlight bulk rupture characteristics.

Synthetic tests

M_w=9.31	M_w=8.1	M_w=8.1	M_w=8.8
(T_r, L)=(545s,1140km)	(T_r, L)=(90s,240km)	(T_r, L)=(60s,220km)	(T_r, L)=(230s,600km)

Point source inversion

				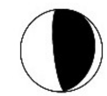
	SAW12D	SAW12D	SAW12D	SAW12D
$\Delta\phi(^0)$	-5.18	-0.36	0.33	-9.06
$\Delta\delta(^0)$	-0.26	2.46	-0.15	1.07
$\Delta\lambda(^0)$	-20.30	4.83	0.18	-9.28
ΔM_w	0.05	0.01	0.00	-0.02
	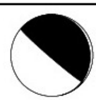	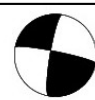		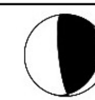
misfit	0.05398	0.00065	0.00060	0.00876

					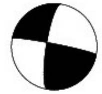						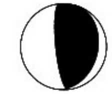	
	SAW12D WN	PREM	PREM WN	SAW12D WN	PREM	PREM WN	SAW12D WN	PREM	PREM WN	SAW12D WN	PREM	PREM WN
$\Delta\phi(^0)$	-0.76	-4.20	-8.81	-0.70	2.16	1.47	2.86	-5.38	-14.33	-0.07	-1.64	-1.44
$\Delta\delta(^0)$	-1.72	-4.29	-4.45	5.73	-0.89	4.26	-0.64	-0.86	-13.08	5.19	7.76	-10.88
$\Delta\lambda(^0)$	-2.17	6.83	-8.02	7.98	-3.19	6.49	-6.97	0.11	6.50	1.29	-8.10	-3.10
ΔM_w	0.07	0.19	0.17	0.00	0.01	0.02	0.01	-0.00	-0.13	-0.09	-0.15	0.12
$\Delta T_r(s)$	0.03	84.59	84.69	-1.91	90.00	90.00	-1.44	60.00	60.00	-0.31	153.91	154.22
$\Delta L(km)$	20.32	-21.13	16.90	121.76	30.71	149.96	93.22	141.88	45.41	131.40	137.25	26.66
						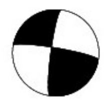			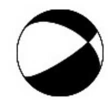	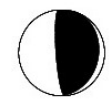	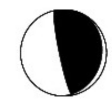	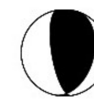
misfit	0.00002	0.01775	0.01777	0.00343	0.02256	0.02438	0.00071	0.01582	0.01990	0.00010	0.02093	0.02098

	SAW12D WN	PREM	PREM WN	SAW12D WN	PREM	PREM WN	SAW12D WN	PREM	PREM WN	SAW12D WN	PREM	PREM WN
$\Delta\phi(^0)$	-7.94	-4.46	-8.11	-0.54	0.23	0.03	2.60	-3.30	0.62	-1.38	-7.35	-1.28
$\Delta\delta(^0)$	-0.15	0.49	-4.86	1.79	3.25	5.19	9.58	1.13	12.67	4.71	2.02	-1.17
$\Delta\lambda(^0)$	-25.78	-15.82	-23.06	3.89	5.56	7.54	7.83	-1.57	8.11	-3.05	-11.15	-5.00
ΔM_w	0.02	0.03	0.19	0.00	0.02	0.01	0.01	0.01	0.02	-0.07	-0.04	0.02
	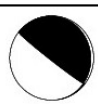	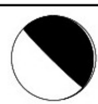	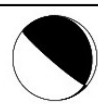	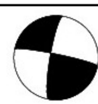	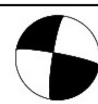	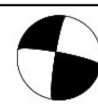				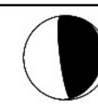	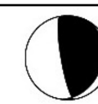	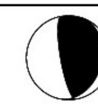
misfit	0.05416	0.05591	0.05609	0.02183	0.05126	0.07130	0.00669	0.02814	0.03401	0.00974	0.02604	0.02702

Error in origin time	+10 s	+0 s	+0 s	+0 s	+0 s	+10 s
Error in latitude	$+0^0$W	$+0^0$W	$+1^0$W	$+0^0$W	$+1^0$E	$+0.60^0$W
Error in longitude	$+0^0$S	$+1^0$S	$+0^0$S	$+1^0$N	$+0^0$S	$+0.23^0$N
	SAW12D	SAW12D	SAW12D	SAW12D	SAW12D	PREM WN
$\Delta\phi(^0)$	-1.83	-5.52	3.45	5.80	-0.88	9.46
$\Delta\delta(^0)$	0.05	4.34	1.4	-6.30	-3.18	-2.71
$\Delta\lambda(^0)$	-2.47	-14.00	7.74	-10.58	-2.02	-4.54
ΔM_w	-0.01	-0.39	-0.07	0.21	0.12	0.12
$\Delta T_r(s)$	-7.96	0.12	0.23	0.62	-0.18	70.91
$\Delta L(km)$	-190.01	-196.32	6.20	-21.90	29.21	-192.97
	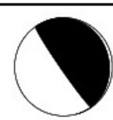	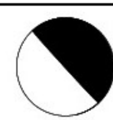	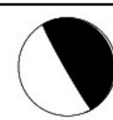	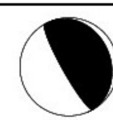	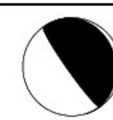	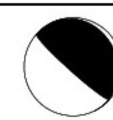
misfit	0.00884	0.00016	0.00349	0.00030	0.00011	0.02209

		$\phi(^o)$	$\Delta\phi(^o)$	$\delta(^o)$	$\Delta\delta(^o)$	$\lambda(^o)$	$\Delta\lambda(^o)$	M_w	ΔM_w
GCMT		329.0	–	8.0	–	110.0	–	9.0	–
This study	GCMT location, (h=28.6km)	343.7	336.5–348.8	19.3	12.8–21.8	121.2	109.2–129.4	9.0	9.0–9.1
This study	GCMT location, (h=10km)	342.5	332.8–345.6	17.0	16.6–28.5	119.3	101.7–120.3	9.0	8.9–9.0
This study	Tsai et al. (2005) Centroid location	340.1	335.0–341.1	10.3	10.1–13.8	113.4	107.0–116.0	9.2	9.1–9.2

Application to real earthquakes

		$\phi(^o)$	$\Delta\phi(^o)$	$\delta(^o)$	$\Delta\delta(^o)$	$\lambda(^o)$	$\Delta\lambda(^o)$	M_w	ΔM_w	$T_r(s)$	$\Delta T_r(s)$	$L(km)$	$\Delta L(km)$
1	GCMT	329.0	–	8.0	–	110.0	–	9.0	–	–	–	–	–
	This study	343.7	336.5–348.8	19.3	12.8–21.8	121.2	109.2–129.4	9.0	9.0–9.1	–	–	–	–
	This study	340.9	309.0–346.8	8.2	6.9–30.4	102.8	90.5–115.7	9.3	8.9–9.3	521.0	480.1–544.3	1276.8	1122.6–1322.5
2	GCMT	203.0	–	10.0	–	88.0	–	9.1	–	–	–	–	–
	This study	202.1	195.5–202.7	9.6	7.1–11.1	98.2	91.5–98.7	9.1	9.0–9.1	–	–	–	–
	This study	197.3	189.1–209.1	9.1	9.0–19.8	79.3	68.2–102.2	9.0	8.8–9.0	151.0	133.5–197.2	461.0	448.5–559.0
3	GCMT	19.0	–	18.0	–	116.0	–	8.8	–	–	–	–	–
	This study	13.6	8.6–20.0	14.8	12.0–21.9	110.5	109.0–119.4	8.8	8.7–8.9	–	–	–	–
4	GCMT	333.0	–	8.0	–	118.0	–	8.6	–	–	–	–	–
	This study	341.0	334.7–341.8	9.4	6.2–13.8	132.8	122.8–133.2	8.7	8.5–8.7	–	–	–	–
5	GCMT	328.0	–	9.0	–	114.0	–	8.5	–	–	–	–	–
	This study	329.6	321.1–333.8	8.1	7.7–19.3	111.7	97.6–116.7	8.6	8.3–8.6	–	–	–	–

1. Sumatra 2004
2. Tohoku 2011
3. Chile 2010
4. Sumatra 2005
5. Sumatra 2007

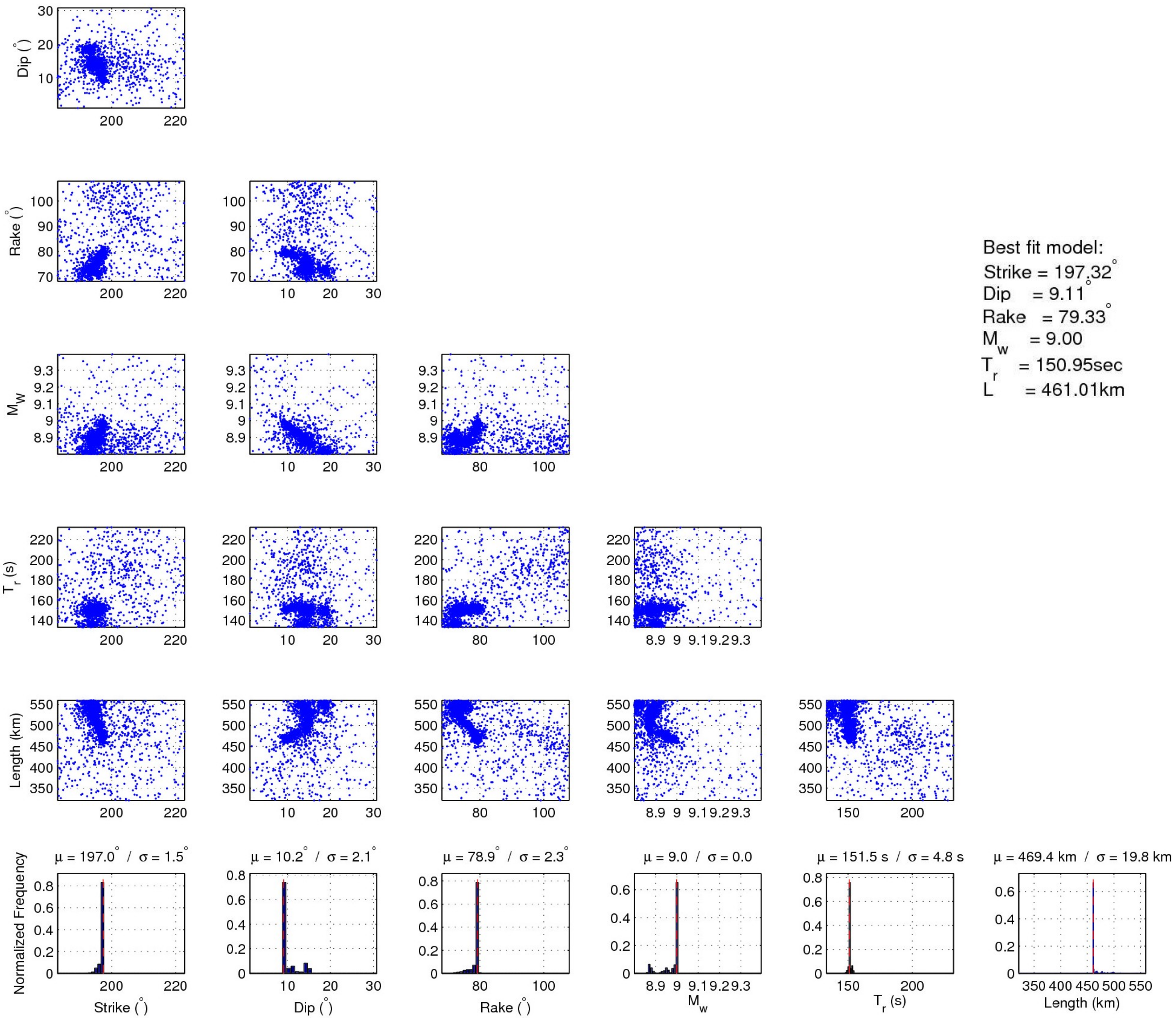

Dip (°)
Rake (°)
M_W
T_r (s)
Length (km)
Normalized Frequency
Best fit model:
Strike = 197.32°
Dip = 9.11°
Rake = 79.33°
M_w = 9.00
T_r = 150.95sec
L = 461.01km
μ = 197.0° / σ = 1.5°
μ = 10.2° / σ = 2.1°
μ = 78.9° / σ = 2.3°
μ = 9.0 / σ = 0.0
μ = 151.5 s / σ = 4.8 s
μ = 469.4 km / σ = 19.8 km
Strike (°)
Dip (°)
Rake (°)
M_w
T_r (s)
Length (km)

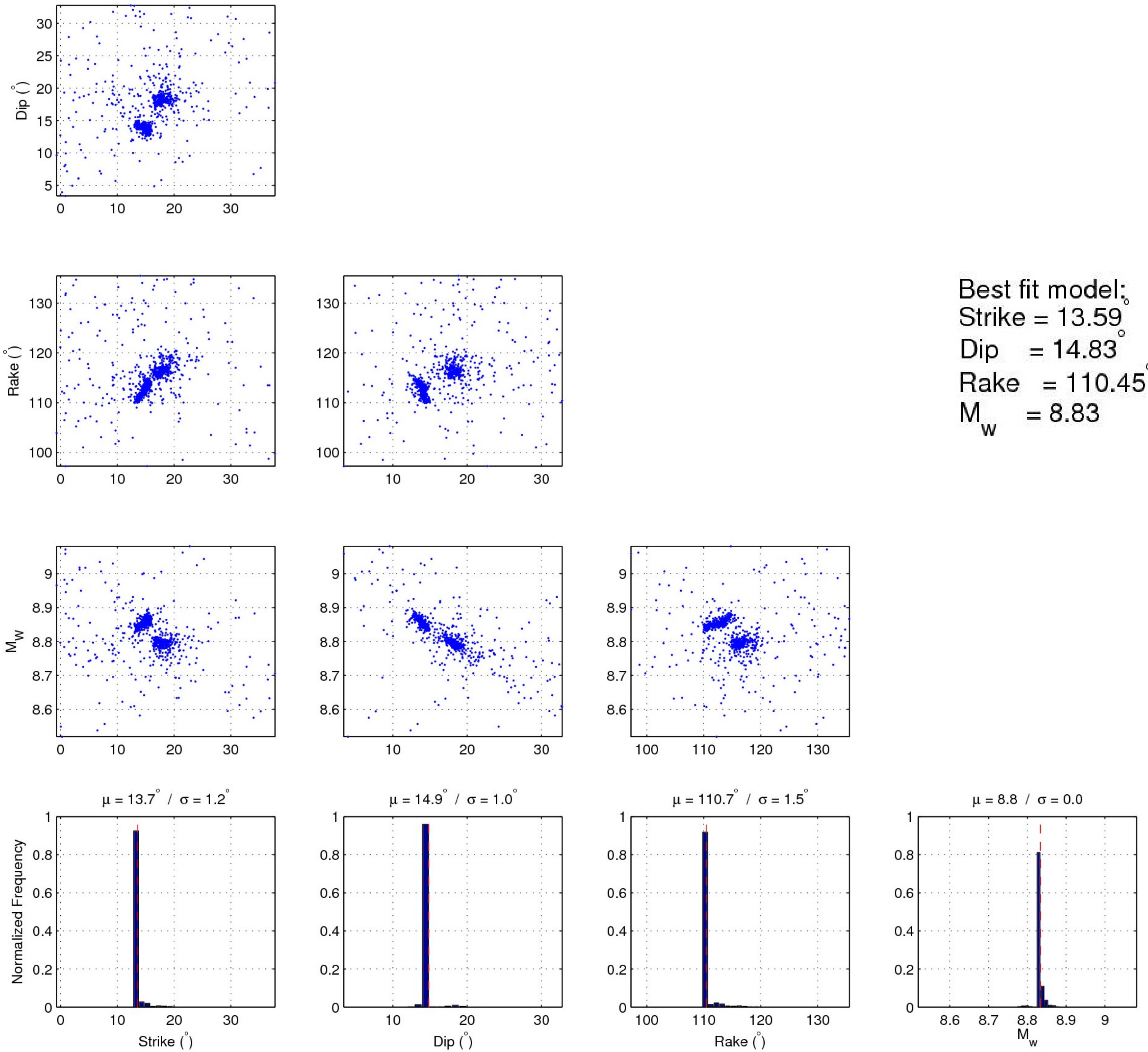
Best fit model:
Strike = 13.59°
Dip = 14.83°
Rake = 110.45°
Mw = 8.83
μ = 13.7° / σ = 1.2°
μ = 14.9° / σ = 1.0°
μ = 110.7° / σ = 1.5°
μ = 8.8 / σ = 0.0
Dip (°)
Rake (°)
MW
Normalized Frequency
Strike (°)
Dip (°)
Rake (°)
Mw